EXPERIMENTAL AND THEORETICAL INVESTIGATIONS OF MICROWAVE HEATING

A Thesis

by

BHAGAT CHANDRA KOTA

Submitted to the Office of Graduate Studies of
Texas A&M University
in partial fulfillment of the requirements for the degree of

MASTER OF SCIENCE

December 2003

Major Subject: Mechanical Engineering

EXPERIMENTAL AND THEORETICAL INVESTIGATIONS OF MICROWAVE HEATING

A Thesis

by

BHAGAT CHANDRA KOTA

Submitted to Texas A&M University
in partial fulfillment of the requirements
for the degree of

MASTER OF SCIENCE

Approved as to style and content by:

K Rajagopal (Co-Chair of Committee)	Jerald Caton (Co-Chair of Committee)
Jay Walton (Member)	Dennis O'Neal (Head of Department)

December 2003

Major Subject: Mechanical Engineering

ABSTRACT

Experimental and Theoretical Investigations of Microwave Heating. (December 2003)
Bhagat Chandra Kota, B. Tech, Indian Institute of Technology, Madras, India
Co-Chairs of Advisory Committee: Dr. K. R. Rajagopal
Dr. Jerald A. Caton

In this work we proposed the governing equations for describing the microwave heating process where the complex interactions between the thermo-mechanical and electro-magnetic fields are taken into account. Starting point are the general balance laws of mechanics and electrodynamics. Transient and spatial temperature profiles of liquids (water and corn solution) inside a cylindrical container during microwave heating at 2450 MHz were measured. Transient temperature rise at a given location was almost linear. The slowest heating region was at the container bottom due to small energy penetration through the bottom. Numerical simulations were carried out for microwave heating of 2-D cylinders of pure water with internal convection in the liquid regions. The results are found to be consistent with those of the experiments. A generalized theoretical model was formulated for the process of microwave heating of materials. Finally stability analysis was done on a 1-D model of microwave heating and the equations for the perturbations were obtained.

DEDICATION

To my parents

ACKNOWLEDGEMENTS

I would like to express my heartfelt gratitude to my advisors, Dr. Kumbakonam Rajagopal and Dr Jerald Caton, for excellent guidance and motivation. Their patience and encouragement during the study has been a source of inspiration for me. I would like to thank my committee member, Dr. Jay Walton, for his suggestions and review of my work. I would also like to thank Dr Lui Tao without whose help and guidance this work wouldn't have been completed.

I would like to thank all my friends especially Vamsee Satish for giving me constant motivation and encouragement. Finally and most importantly thanks are due to my parents, sister and Swapna for their support and encouragement.

TABLE OF CONTENTS

Page

Page

LIST OF TABLES

Page

LIST OF FIGURES

Page

Page

INTRODUCTION AND OBJECTIVES

1.1 Introduction

Microwaves with their ability to rapidly heat dielectric materials are commonly used as a source of heat. In the food industry microwaves are used for heating, drying, thawing, tempering, sterilization etc. The number of applications using microwave radiation as a source of thermal energy has increased in the recent past, mainly due to two major advantages over conventional heating techniques: quick start-up periods and the ability to heat a material evenly. Radiation whose frequencies range from 300 MHz to 300 GHz with wavelengths ranging from a few mm to 30 cm are referred to as microwaves and heat effects that occur in this frequency range will be referred to as microwave heating. The temperature distribution in a product submitted to microwave radiation is governed by the interaction and absorption of radiation by the medium and the accompanying transport process due to the dissipation of electromagnetic energy into heat. This phenomenon is described as *Microwave Heating*. Thermal modeling has become very important to optimize heating processes and achieve uniform heating in microwave ovens.

In classical thermodynamics, though radiative heat transfer has been the object of extensive scrutiny for decades, when one strays from the black body radiation, which is an idealization of very limited applicability, we enter into ad hoc formulae that apply to real materials that involve ad hoc factors to fit one experiment or another. There is no systematic theory in place to distinguish the manner in which different materials convert the electromagnetic radiation into energy in its thermal form, i.e., there is no reasonable constitutive theory in place for radiative heat transfer. Moreover, classical thermodynamics is not well suited to the study of inhomogeneous bodies where the conversion of the electromagnetic radiation can differ from one material point in the body to another. An interesting application where such information is critical is for instance

---

This thesis follows the style and format of *AIChe Journal*.

laser surgery of inhomogeneous biological materials (Rajagopal and Tao, 2002). Characterization of the energy deposition and physical changes taking place in materials during the microwave heating process requires solution of the electromagnetic and energy transport equations. While lumped and uniform energy deposition models are useful for understanding the qualitative influence of processing parameters, models which include the temporal and spatial variation of electromagnetic field intensity within a cavity will provide more accurate means for predicting and assessing the heating patterns.

1.2 Objectives

The main objective of this project is to develop a thermodynamic model for microwave heating process that can be applied within the context of a continuum perspective on the basis of some simple experiments conducted on different bodies in a microwave cavity. The efficacy and validity of the theory will be tested on the basis of the solution of some simple boundary value problems and some simple laboratory experiments.

LITERATURE SURVEY

Over the years many researchers have proposed many theories and models on microwave heating. Some of the early work, which used Maxwell's equations to deduce electric field distributions in single and multilayered slabs, was concerned with assessing the effects of microwaves and radio frequencies on biological tissues. These studies were primarily concerned with electric field distributions in the sample. However the influence of sample dimensions and dielectric properties on the internal fields weren't investigated. Much of the early work on microwave heating was based on Lambert's law formulation for the absorbed microwave power. This approach was used by Ohlsson and Bengtsson (1971), Mudgett (1986) and Chen et al., (1993). These studies are restricted to one-dimensional conduction and the dielectric and thermal properties are assumed to be independent of temperature. Barringer et al., (1995) and (1994) conducted experiments on the heating of slabs exposed to microwave s and compared the temperature distributions with the power predicted form the Maxwell's equations.

Significant contributions were also made in solving for the temperature distribution numerically. Lin et al., (1995) used a finite element technique to predict the temperature distribution in model foods of cylindrical and rectangular shapes during microwave heating. Chen et al., (1993) did finite element formulation for the analysis of temperature distribution in a microwaved potato cylinder. Zhao and Turner (2000) used a finite volume time domain (FVTD) technique to solve the coupled equations. Clemens and Saltiel (1995) and Haala and Wiesbeck (1996) used Finite difference time domain (FDTD) technique to solve the coupled Maxwell's equations. A comparison of power distribution obtained by solving Maxwell's equation to that by using Lambert's law was presented by Olivera and Franca (2002). Effects of sample size, sample rotation, microwave frequency and variation of radiation angle were examined.

The literature concerned with microwave heating of materials with temperature dependent properties is sparse. In most food samples the dependence of dielectric properties on temperature is greater at lower frequencies. Most of the literature on microwave heating in 3D is restricted to power absorption and heating in homogeneous and multilayered spheres. Ohlsson and Risman (1978) have conducted microwave-

heating experiments at 2,450 MHz on spherical and cylindrical samples. Pronounced heating in the center of the object was observed for spheres and cylinders with diameters in the range of 2-6 cm and 1.8-3.5 cm respectively. In a study by Barringer et al., (1994), heating rates of cylindrical samples of oil and water were compared. Ayappa et al., (1991a) and (1991b) investigated the power distributions in cylinders and slabs by calculating the average power absorbed by the sample.

Many groups have completed significant research on the effect of microwave heating on samples of water. Ayappa et al., (1994a) and (1994b) investigated natural convection of a liquid in a square cavity exposed to microwaves at a frequency of 2,450 MHz. Convection effects within the sample were take into consideration. Natural convection in a fluid with a uniform heat source has been studied by Gartling (1982) and (1977), Lambha et al., (1978) and Jahn and Reineke (1970). Datta and Prosetya (1991) conducted experiments on heating of oil and water at 2,450 MHz. Heating in a 500 cc container whose top and bottom were covered with aluminum foil showed pronounced center heating with cooler liquid at the bottom of the vessel. A similar effect was observed by Ayappa et al., (1992) and (1994a). Datta et al., (1992) modeled the microwave heating of water in a 2000 cc vessel placed in a commercial oven. The momentum, continuity and energy equations were solved using finite difference scheme with Lambert's law approximation to the microwave power. Barringer et al., (1995a) investigated the heating rates of various oil-in-water and water-in-oil emulsions. It was found that the emulsions heated faster than the corresponding layers. Ayappa and Basak (1997), (2001) and (2002) presented finite element solutions for microwave thawing using a 2-D model for infinite cylinders exposed to plane electromagnetic waves and also illustrated the efficacy of using the effective heat capacity model to solve the problem. Datta and Zhang (2000) investigated thawing of foods in a microwave oven and also made observations on the effect of power cycles, power levels, load geometry and dielectric properties on the temperature response.

Rajagopal and Tao (2002) proposed a thermodynamic framework for describing the microwave drying process of aqueous dielectrics using Maxwell-Lorentz field equations and mixture theory. Rajagopal and Wineman (1992) developed a three-dimensional continuum model for an electrorheological fluid trapped between two plates

where they assumed that the electric field is constant in the gap where the material is entrapped. However by doing so, the electric field enters the problem purely as a parameter. Lin et al., (1995) conducted experiments to investigate the effect of viscosity and salt concentration on microwave heating of model Non-Newtonian liquid foods in a cylindrical container.

EXPERIMENTAL SETUP

3.1 Microwave Oven and Temperature Sensors:

The microwave oven used in this work is a Sharp (R-530EK) domestic microwave oven with cavity dimensions 60.8-cm x 34-cm x 48.7-cm. As shown in figure 3.1 and figure 3.2, food samples were placed at the center of the microwave cavity. The microwave has a maximum power output of 1200 watt and it has the option of eleven preset power levels. The power levels used for this study were 360, 600, 840 and 1200W, respectively. Figure 3.1 shows the schematic layout of the microwave.

3.2 Test Materials:

The test samples include water and corn starch solution and they were placed in a beaker with dimensions of 7.4cm (diameter) x 8.5cm (height). The test samples will be placed at the center of the microwave cavity with the turntable absent.

3.3 Data Acquisition Module:

The time temperature data were collected using OMEGABUS D5000 series transmitter. The D5000 four channel sensor to computer modules are a family of complete solutions designed for data acquisition systems based on personal computers and other process based equipment's with standards I/O ports. The module converts four analog input signals to engineering units and transmits in ASCII format to any host with standard RS-485 or 232C ports. The maximum number of channels for temperature measurement was limited to four. The unit was interfaced to a personal computer via an RS 232 serial port.

3.4 Data Acquisition Software:

In order to get continuous temperature time data DASY lab V6.0 module software was used for data acquisition. Data acquisition hardware is connected to DASY Lab through the RS 231 module. The data can be exchanged between DASY lab and other windows application via DDE.

3.5 Thermocouples:

Precision fine wire thermocouples from Omega (5TC-TT-K-24-36) were used to measure temperature at various locations within the test samples. The thermocouples were made from Nickel Chrome alloy and the diameter was around 0.02 inch. These are usually insulated with PFA Teflon. The response time of these thermocouples was found by performing some simple experiments.

3.6 Microwave Power Efficiency Calculation:

Microwave efficiency was calculated by comparing the time it takes for a beaker of water to reach the boiling point with that when the total power is used to heat up the water.
Time taken by the microwave to heat the water to boiling point = 95 seconds.
Wt of water taken = 0.345kg; initial temperature = 24C; final temperature = 100C

$$E = mc_p \Delta t$$

= 110.88 kJ

Maximum power of the Microwave = 1200W
Let t be the time it would take if maximum power output was used.

Then $t = \frac{110.88}{1200}$ = 92.40 seconds.

Hence we can assume that the microwave uses essentially all the power to heat up the sample.

Figure 3.2 shows the actual experimental setup with all the connections made.

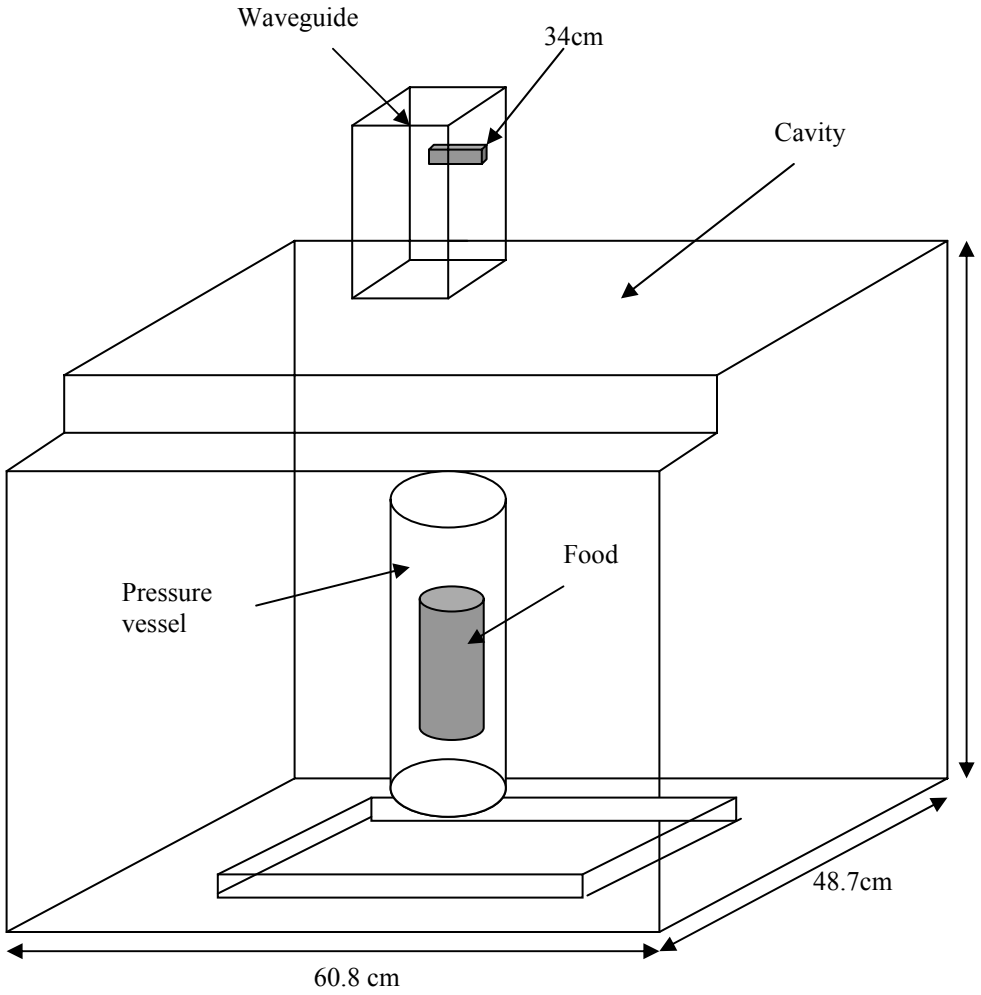

Figure 3.1 Schematic Layout of Microwave Oven

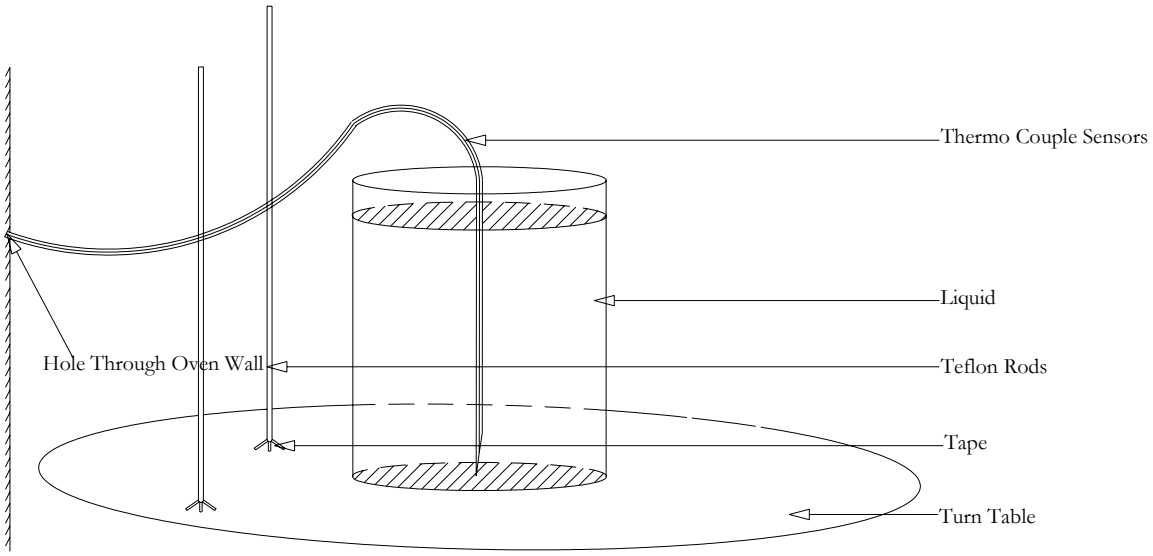

Figure 3.2 Experimental Set-up

RESULTS AND DISCUSSION

4.1 Experimental Procedure

The samples were taken in variable amounts in the test beaker and the thermocouples were attached at fixed locations inside the test beaker. The microwave run time is set to a fixed time depending on the sample. The microwave and the data acquisition are switched on simultaneously to record data. Each experiment is repeated several times to get accurate data. Experiments are also repeated to account for the effect of

1. sample size
2. location of sample in the cavity
3. microwave power

4.2 Experimental Results

4.2.1 Estimate of the Time Constant of the Thermocouple:

Figure 4.1 shows a typical time response for the thermocouple. The thermocouple was suddenly plunged into a water bath with water at 98C. The ambient air conditions are at 22C. The results show a rapid rise in the temperature, and the first order time constant was estimated to be around 1.6sec. From Figure 4.1 we can observe that the experimental and the calculated values are close.

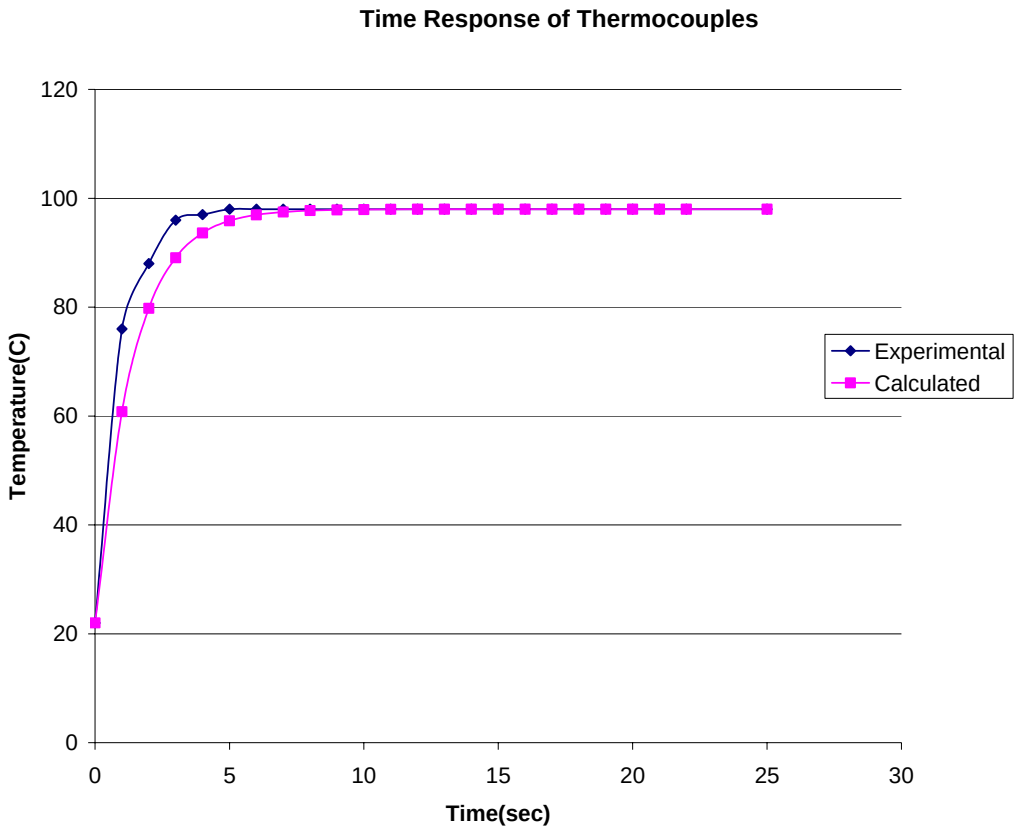

Figure 4.1 Typical Response of a Thermocouple

4.2.2 Numerical Calculation of Time Constant:

To compare the above experimental estimate of the thermocouples time constant, an analytical estimate was completed.

The composition of the thermocouple is 7% Ni, 27% Cr and balance Fe, and has the properties[a] as shown in table 4.1.

Table 4.1 Properties of the Thermocouple

Specific Gravity	7.25
Diameter	.02 inch
Specific Heat of Thermocouple	0.47J/gk
Overall Heat Transfer Coefficient	180 J/m^2Ksec

The first order time constant for a thermocouple is given by the relation

$\tau = \frac{mc}{hA}$ and the time constant is found to be 1.55 seconds.

The slight variation in the experimental and the calculated time constants might be due to the choice of the h value and the geometry approximation. Figure 4.2 and table 4.2 show the variation of the computed time response of the thermocouple with variation of the heat transfer coefficient. It can be seen that the response gets slower as the heat transfer coefficient is decreased and vice versa.

[a] The properties were obtained from Omega Inc. and Heat Transfer by Mills.

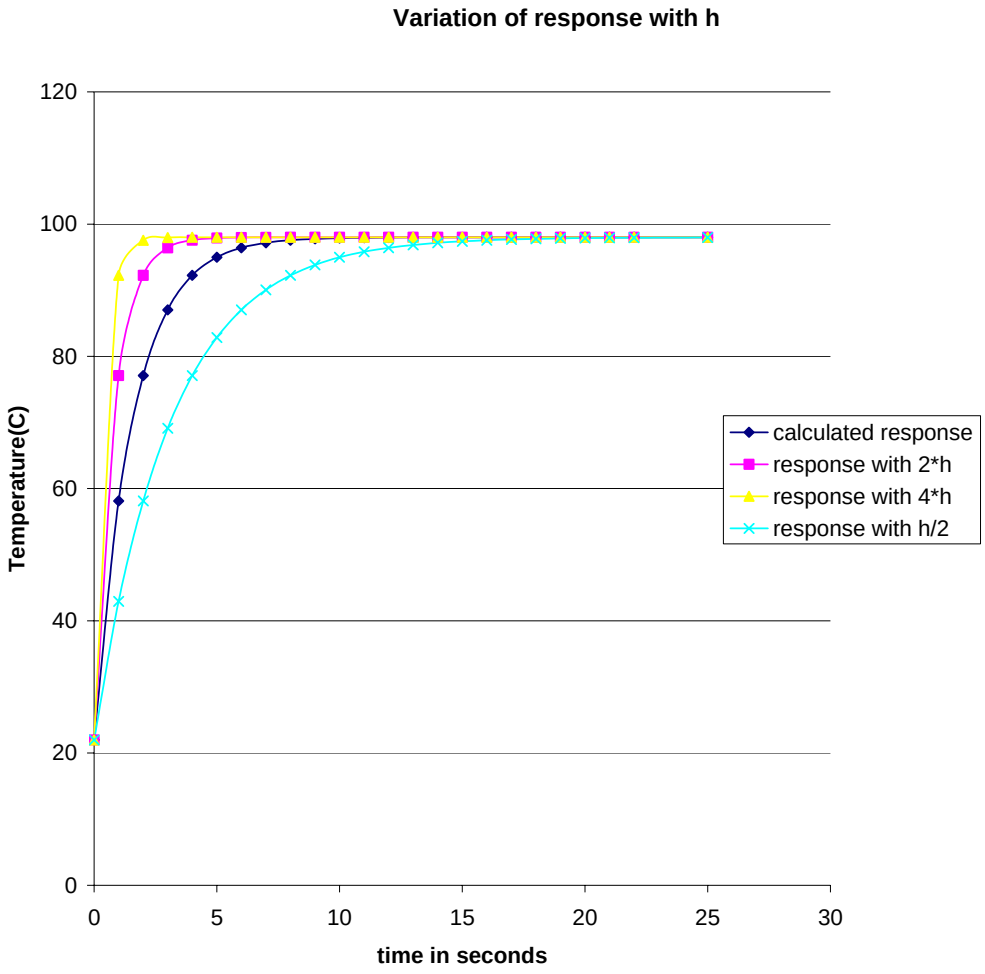

Figure 4.2 Variation of Time Constant with Heat Transfer Coefficient

Table 4.2 Variation of Time Constant with Heat Transfer Coefficient

Heat Transfer Coefficient (J/m^2Ksec)	Time Constant (seconds)
180	1.55
90	3.10
360	0.775
720	0.3875

Table 4.3 and figure 4.3 show the variation of the computed time response of the thermocouple with variation of the diameter. It can be seen that the response gets faster as the diameter is decreased and vice versa.

Table 4.3 Variation of Time Constant with Diameter of Thermocouple Used

Diameter (inch)	Time constant(sec)
0.02	1.55
0.022	1.705
0.018	1.395

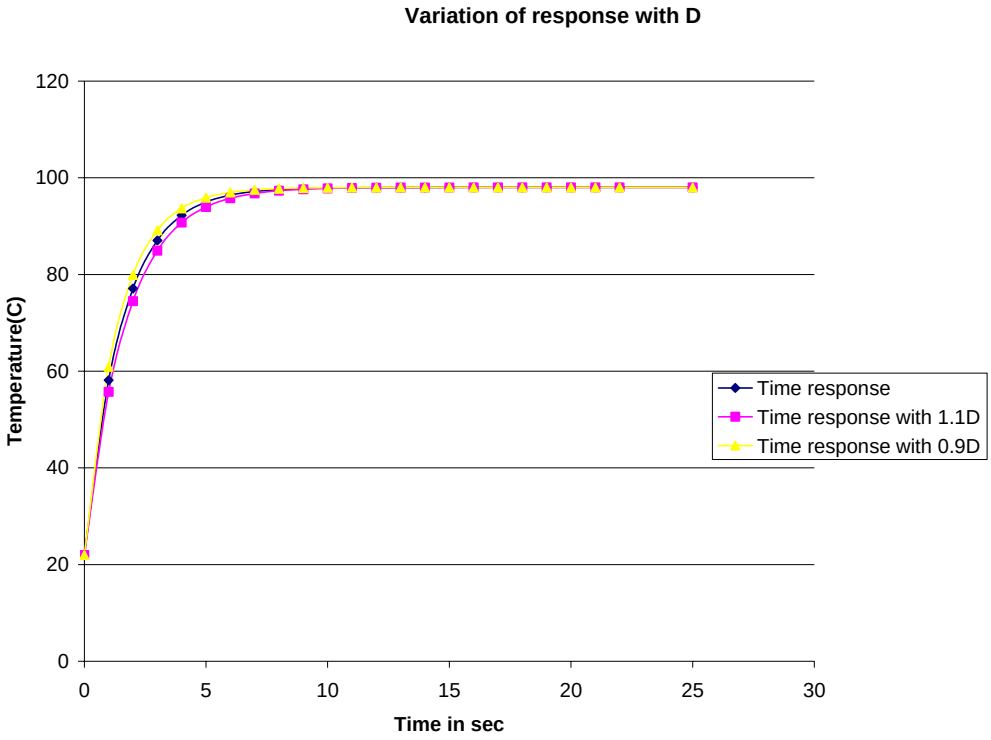

Figure 4.3 Variation of Time Constant with Diameter

4.2.3 Experimental-Matrix:

Experiments were performed to get the time response of the temperatures inside the sample as a function of

- Type of sample being experimented.
- Position of the sensors inside the sample.
- Amount of the sample.
- Power output of the microwave.
- Effect of the turntable.
- Position of the sample inside the microwave.

Initially the experiments were performed using a part of a potato. The samples were cut in the shape of a square and the response was studied. A typical response is as shown in the appendix B. Experiments couldn't be repeated since sparks appeared inside the microwave whenever the potato was used. This might be due to the high dielectric constant of potato. It was decided to perform experiments on three kinds of liquids-water, which is a Newtonian fluid, and two non Newtonian fluids. Of the two non Newtonian fluids, one would be a shear thickening liquid and other would be shear-thinning liquid.

4.2.4 Experiments on Water:

Water was placed in a beaker with dimensions of 2.9” (diameter) x 3.4”(height). The sample was irradiated at maximum power for around 150 seconds and the response was studied. The thermocouple was placed at the bottom of the beaker close to the wall. Figure 4.4 shows the water temperature for three different tests conducted about 15 minutes apart. After a short delay, the water temperature increased until a temperature near 100C was attained. The elapsed time from start of heating until 100 C was attained was between 180-190 seconds in all the three cases. The variation of the time response between experiments is probably due to slight variation in the position and placement of the thermocouple. It can also be due to the difference in the initial oven temperature. From the graph we can observe that the response is initially linear with the temperature increasing with time and then it attains steady state once the water reaches boiling point. The spikes in the graph might be because of sudden spark and also due to the formation of bubbles once the water starts boiling. Experiments were done to study the variation of temperature with position. Since it was tedious to maintain the thermocouples at the center, two thermocouples were fixed one at the bottom near the wall and the other at the top near the surface as shown in figure 4.5.

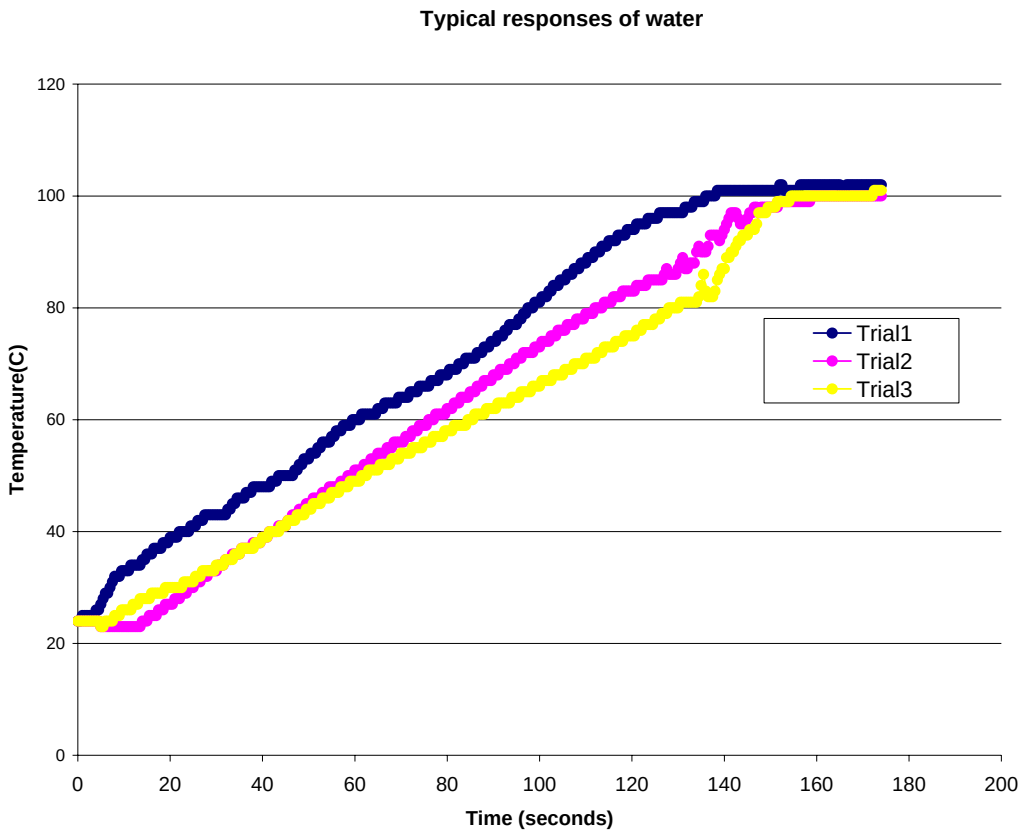

Figure 4.4 Typical Response of Water

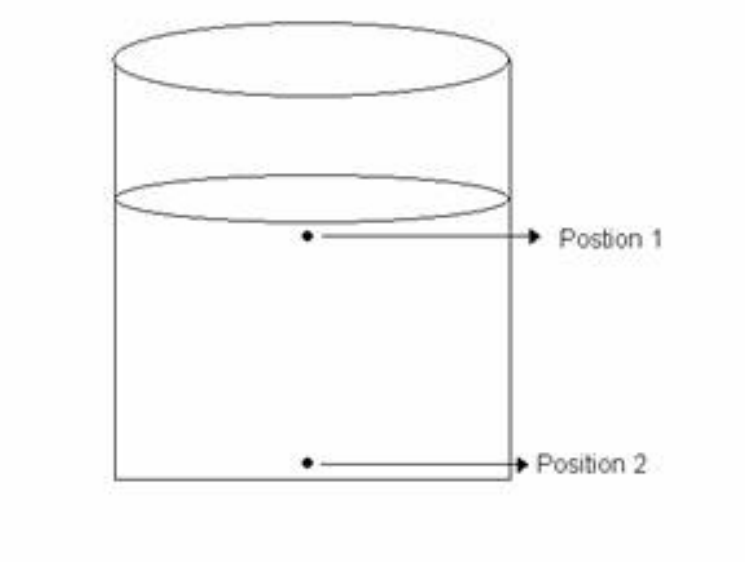

Figure 4.5 Test Apparatus with Thermocouple locations

Figure 4.6 shows the response observed. It can be seen from the response that the top surface heats up more quickly than the bottom surface.

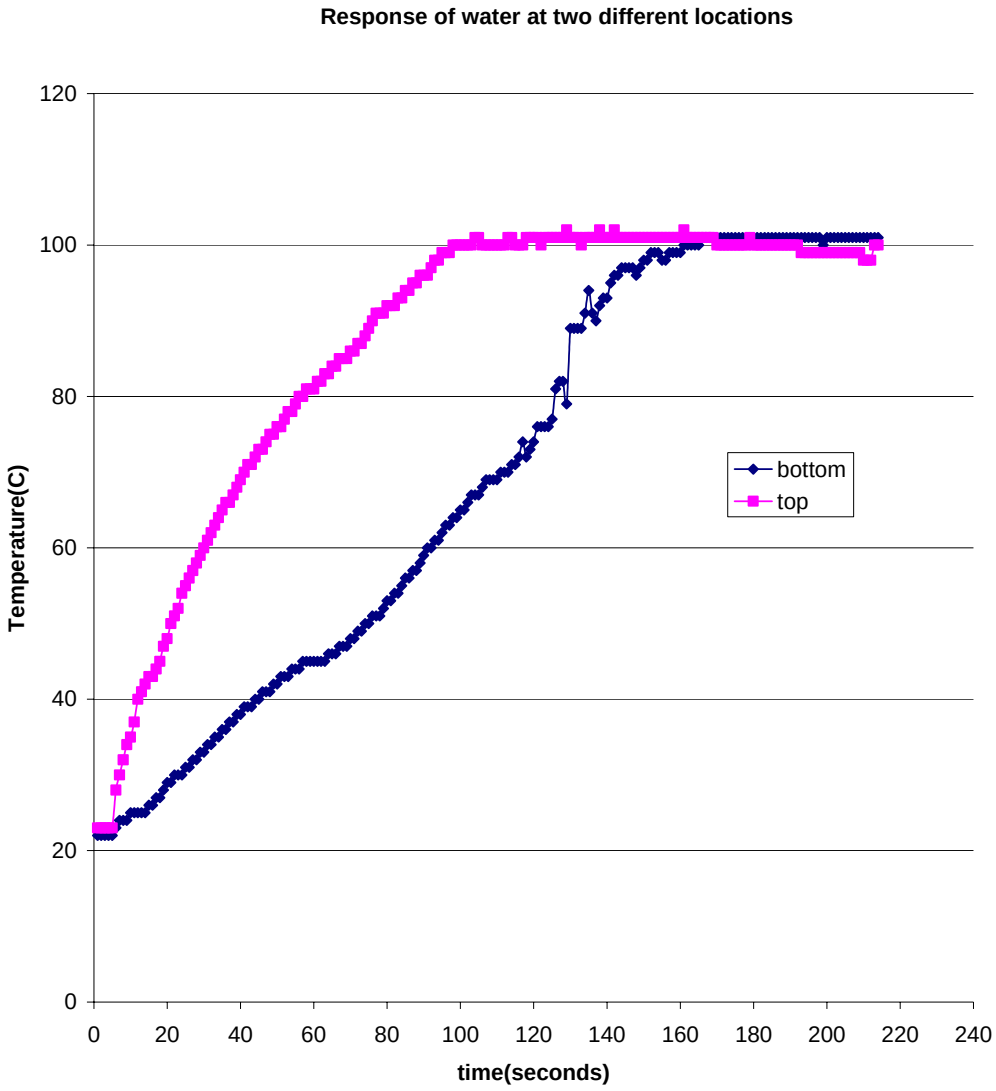

Figure 4.6 Response of Water at Two Different Locations

To study the effect of the position of the sample at an increased height, the beaker was placed on a plastic platform as shown in figure 4.7 and the response was studied.

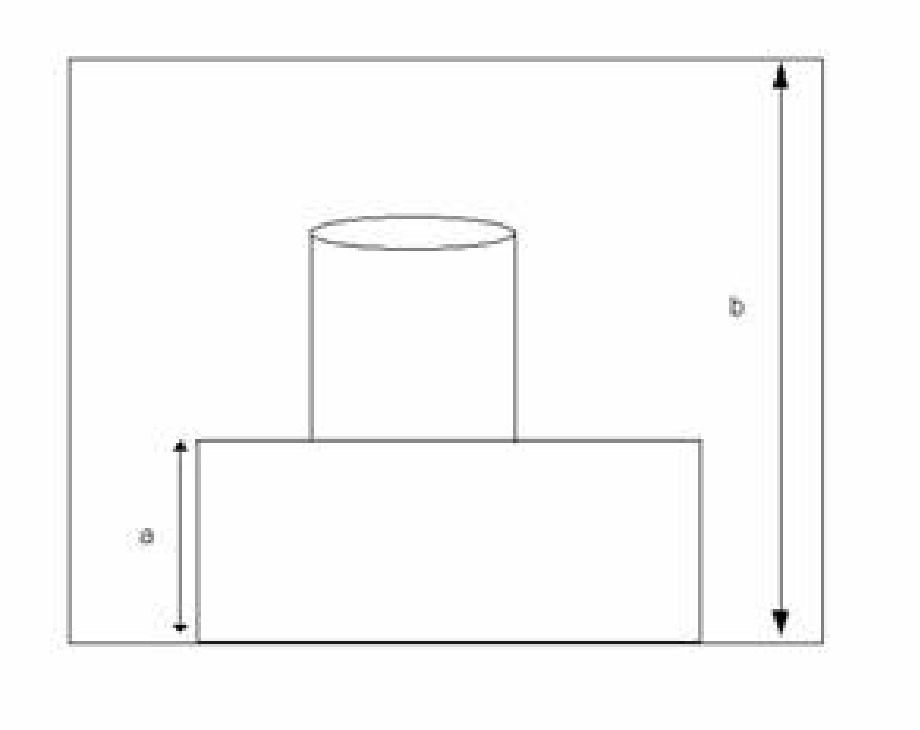

Figure 4.7 Test Apparatus Placed at an Increased Height

Figure 4.8 shows the response observed. It can be seen that the increase in the level did not make any changes in the response. The sudden leap in the response of water when it was placed at a low level might be due to bubbling of water since the top surface has already reached the boiling point.

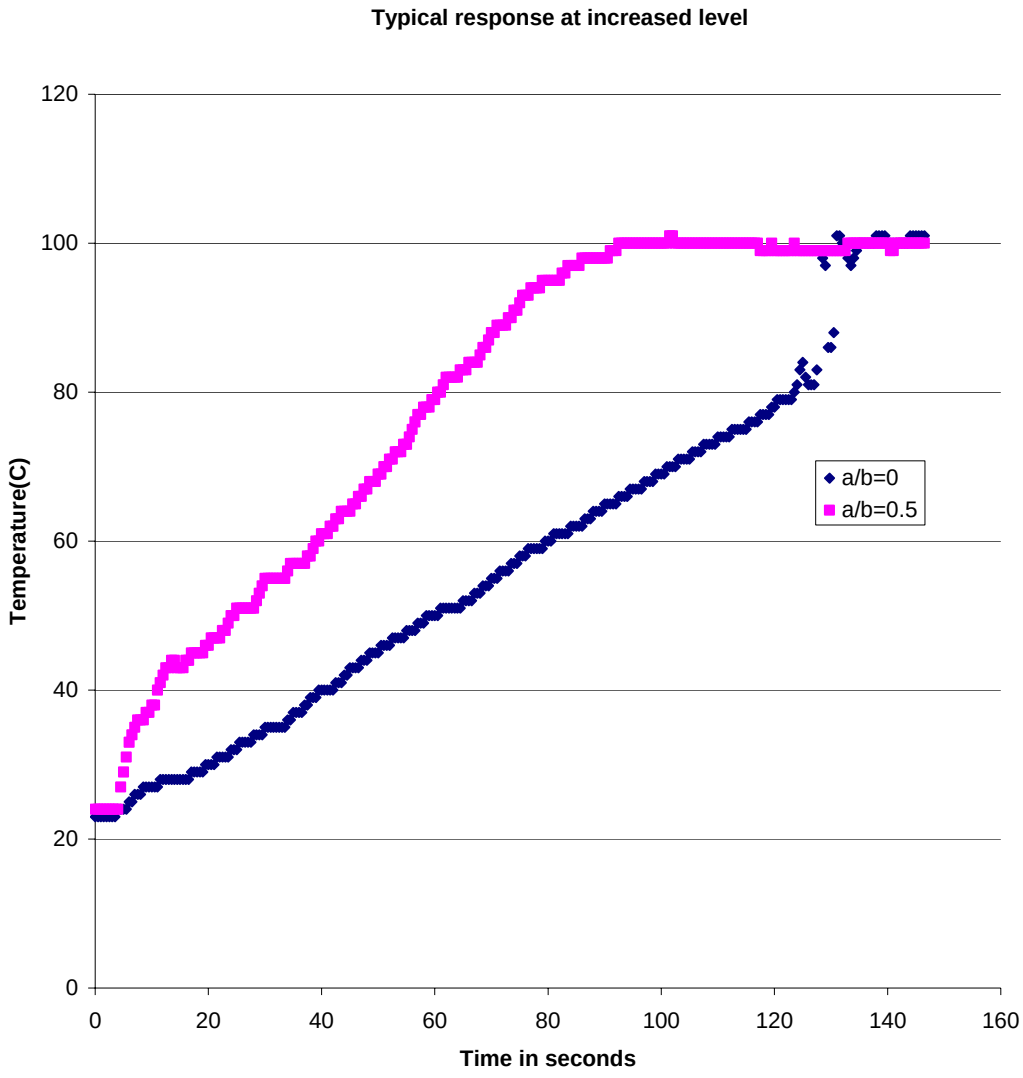

Figure 4.8 Response of Water with Beaker Placed at an Increased Level

Experiments were done to study the effect of position of the sample inside the microwave cavity. The beaker was placed at four different locations inside the microwave oven cavity at the positions as shown in figure 4.9.

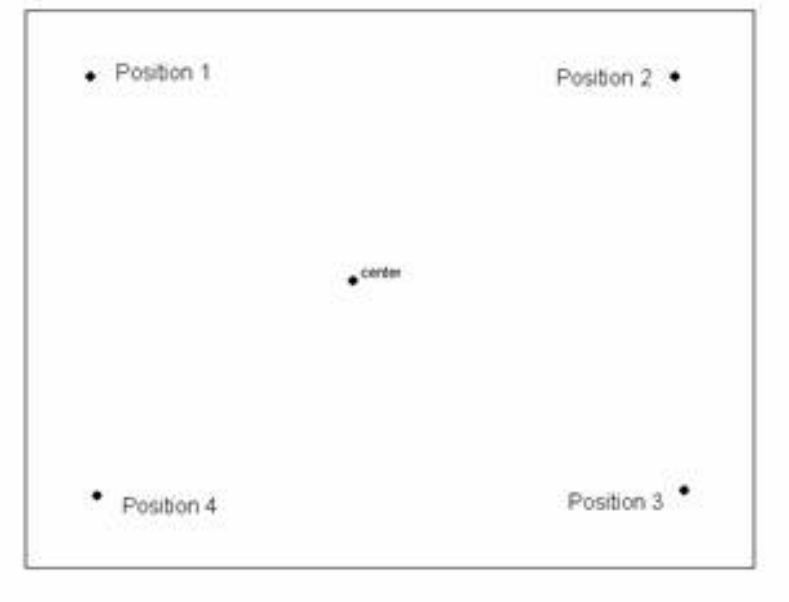

Figure 4.9 Variation of Position of Sample in the Microwave

Figure 4.10 shows the response observed. It can be seen that varying the position of the beaker inside the microwave cavity did not have a significant effect on the response towards microwave heating. There was uniform heating throughout the microwave cavity. Experiments were done at different microwave powers to study the effect of the power on the temperature response. The microwave was operated at power levels of 100%, 70%, 50% and 30% of the maximum power output of the microwave. Figure 4.11 shows the response observed. It can be seen that at higher power levels the sample gets heated up faster than at lower power levels. The On-Off behavior of the microwave at lower power levels can also be seen from the response especially from the response at 30% power. It can be seen from the response that the zone in which the temperature rises is almost 30% of the total cycle zone. Figure 4.12 shows the variation of Temperature with the radial distance from the center. We can see that the center is at a higher temperature than near the surface but the difference is very little.

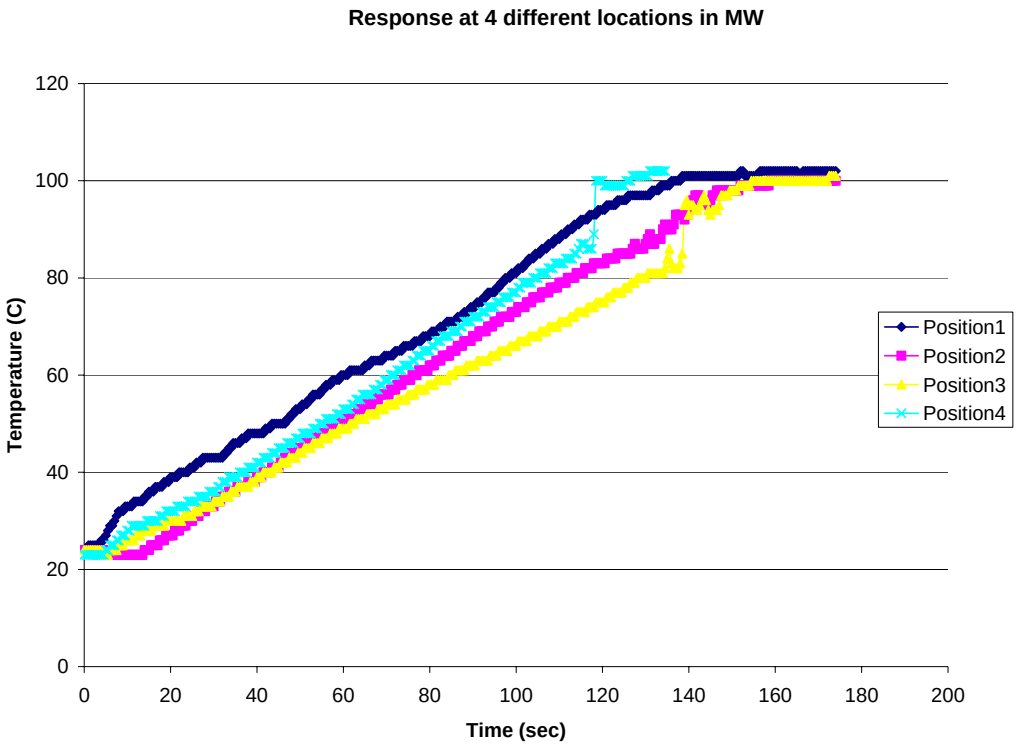

Figure 4.10 Response of Water when Placed at Various Locations in the MW Cavity

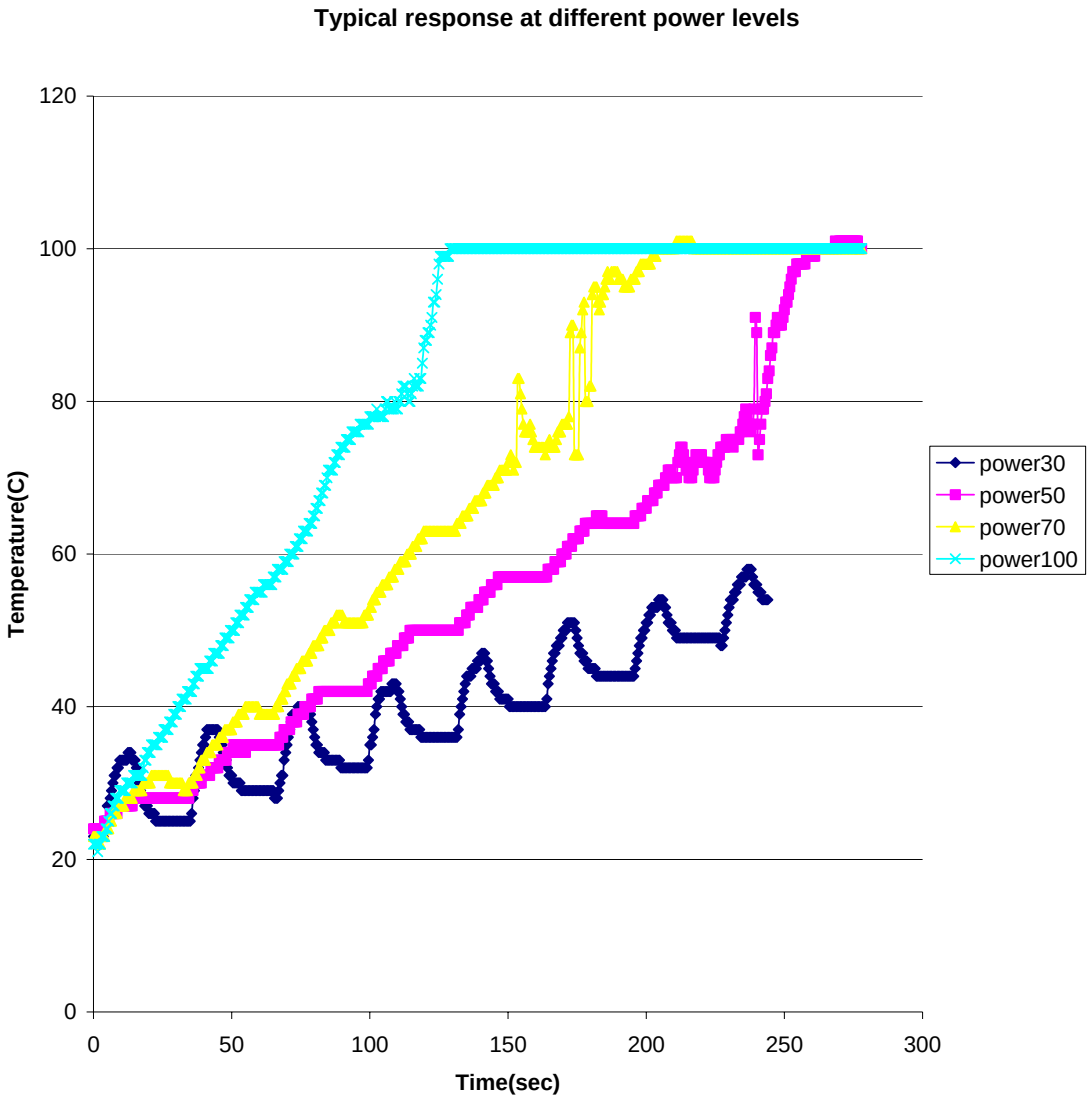

Figure 4.11 Response of Water at Various Power Levels

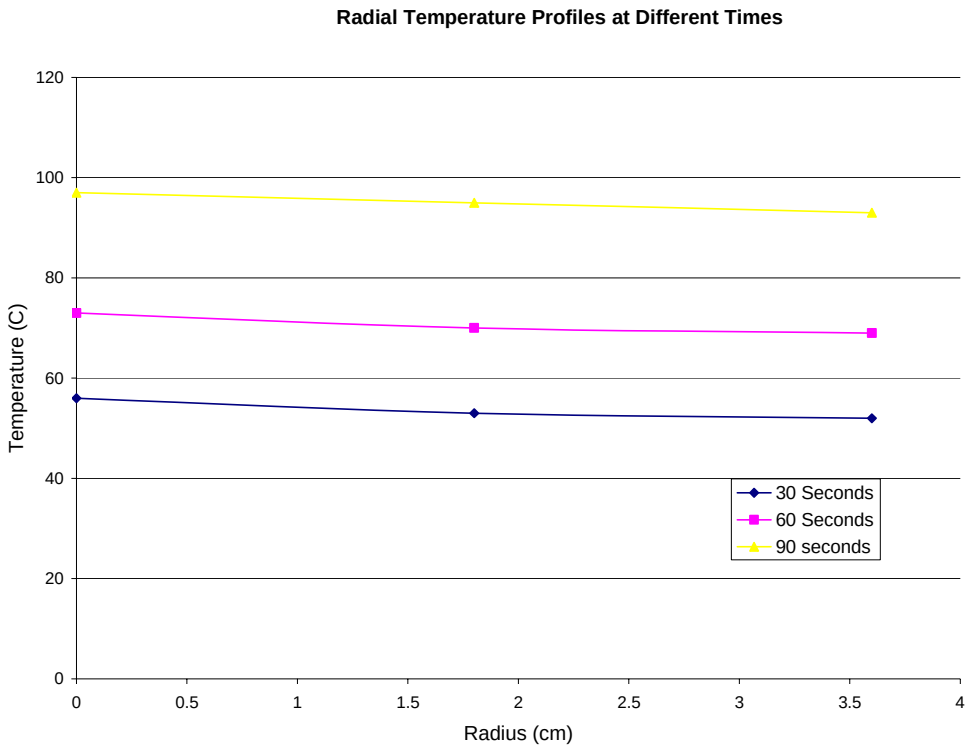

Figure 4.12 Radial Temperature Profiles at Different Times

4.2.5 Experiments with Cornstarch and Tomato Ketchup:

To study the effect of microwave heating on Non Newtonian fluids cornstarch solution which is a shear thickening liquid and tomato ketchup which is a shear thinning liquid were chosen. Experiments were performed using 40 %(by mass) cornstarch solution which would be shear thickening liquid. The same beaker was used as for the experiments with water. About one half of the beaker was filled with cornstarch solution. The thermocouple was placed at the bottom of the beaker and the response was studied. Figure 4.13 shows the response of the temperature in the cornstarch solution and in the water. The experiment was repeated with the same test conditions but at a reduced power to obtain more data points. Figure 4.14 shows response at 50% of the maximum power. Experiments were also performed with domestic tomato ketchup as the test liquid. The experiments were performed in the same beaker and equal volumes of the ketchup as water. Figure 4.15 shows the typical response of tomato ketchup compared to that of water and when the thermocouple is placed at the same location. From the figures we can see that response of cornstarch is almost similar water whereas tomato ketchup heats up a bit faster than water.

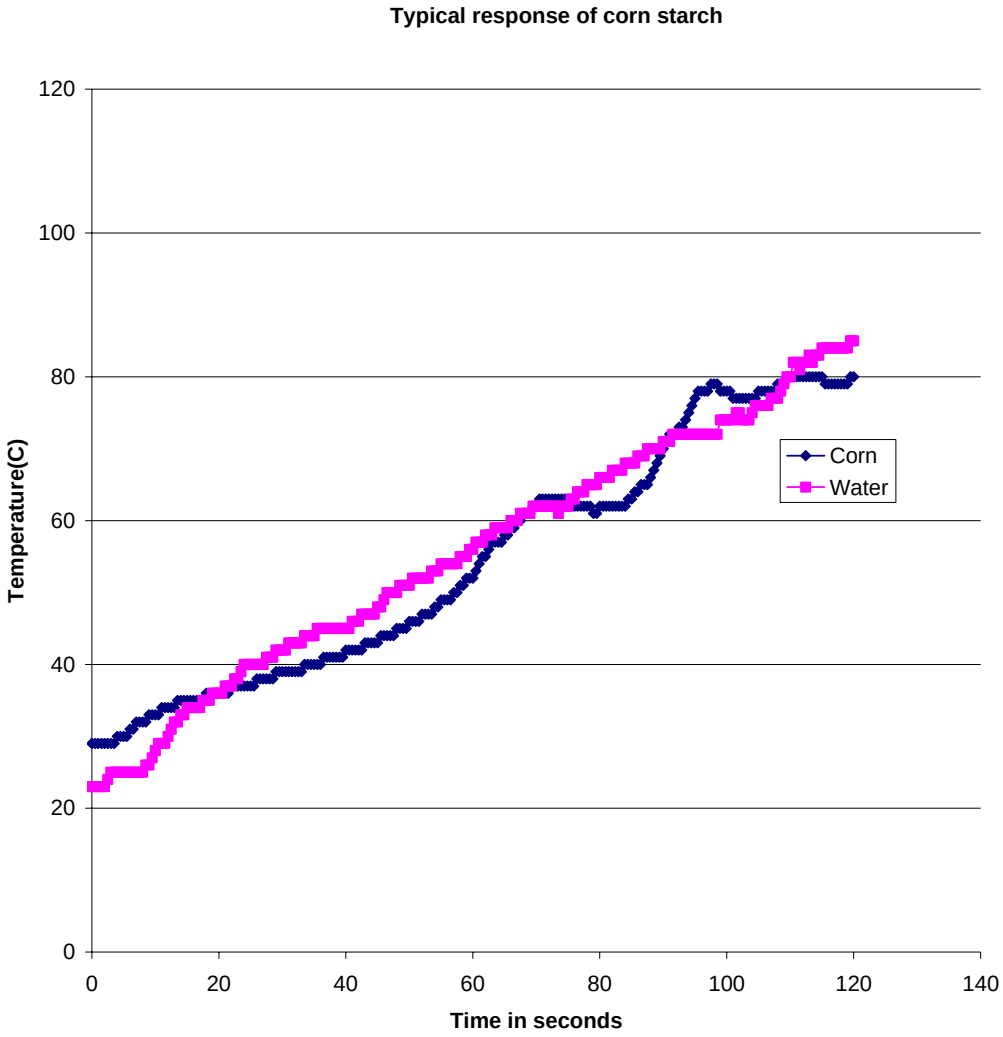

Figure 4.13 Typical Response of Cornstarch against Water

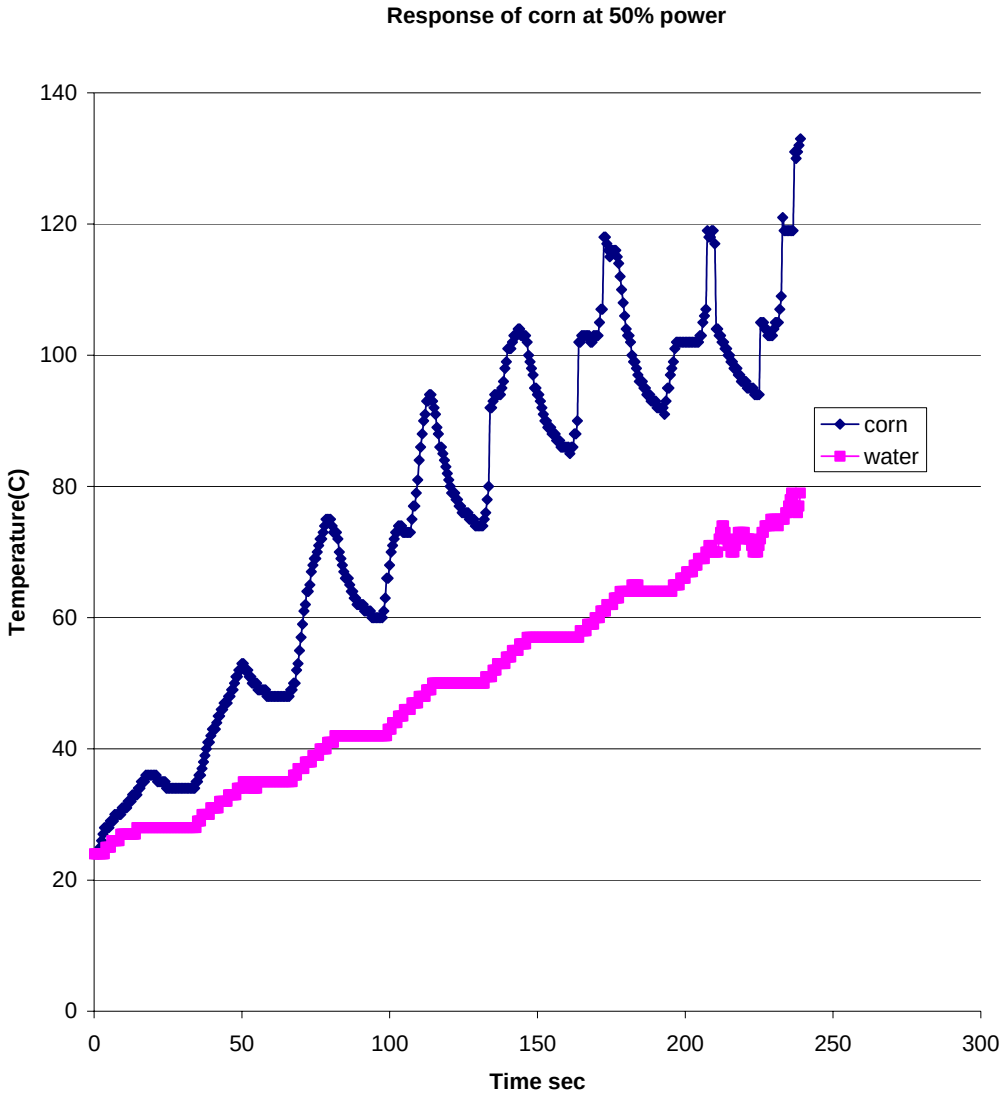

Figure 4.14 Response of Cornstarch at 50% Maximum Power

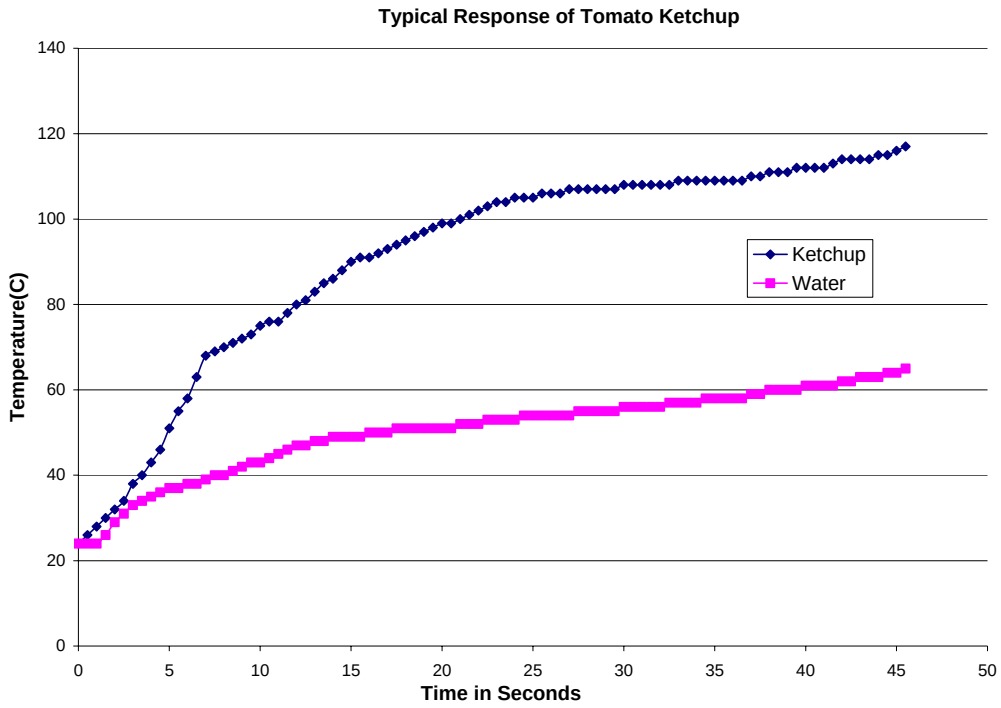

Figure 4.15 Typical Response of Tomato Ketchup

NUMERICAL RESULTS

Numerical Simulations were performed on a square domain (figure 5.1) of side 10 cm containing water. Finite Element software FEMLAB was used to perform the numerical simulations. Suppose this square domain is exposed to a plane wave with its electric field incident first on the bottom of the square domain. Maxwell's equations govern the propagation of electromagnetic wave in the medium. Assuming time dependence for the electric field in the form $e^{-i\omega t}$, the governing equation for the spatial distribution of electric field will be in the form

$$\nabla^2 E + k^2 E = 0, \tag{5.1}$$

where $k = \alpha + i\beta$. The phase constant α and attenuation constant β are related to the dielectric properties of the medium and the frequency of the incident radiation.

5.1 Boundary Conditions:

The electric field and its derivatives are continuous at the boundaries where the radiation enters and leaves the domain. We also assume that there aren't any radiation losses from the sides and initially there is no radiation present in the material so that we have the following boundary and initial conditions.

Boundary condition at the edge where the radiation is incident is

$$\nabla \mathbf{E} + ik\mathbf{E} = 2ik, \tag{5.2}$$

at the other end of the domain

$$\nabla \mathbf{E} + ik\mathbf{E} = 0, \tag{5.3}$$

on the remaining edges we have

$$\nabla \cdot \mathbf{E} = 0, \tag{5.4}$$

The momentum, energy and continuity equations for a Newtonian Boussineq fluid are Respectively:

$$\rho_o \frac{\partial \mathbf{v}}{\partial t} + \rho_o \mathbf{v} \cdot \nabla \mathbf{v} = -\nabla p + \mu \nabla^2 \mathbf{v} + g\rho_o[1 - \beta(T - T_o)], \tag{5.5}$$

$$\rho_o c_p \frac{\partial T}{\partial t} + \rho_o c_p \mathbf{v} \cdot \nabla T = \nabla \cdot k \nabla T + P(r), \tag{5.6}$$

and

$$\nabla \cdot \mathbf{v} = 0. \tag{5.7}$$

The sample boundaries are thermally insulated with no slip and no penetration conditions for the flow. We also assume that the thermal and flow fields are two-dimensional in nature. In all the calculations the initial temperature is assumed to be uniform at 298 K.

Material dielectric and thermal properties of water used in the study are listed in Appendix B.

Figure 5.2 shows the electric field distribution (electric field value in V/m) when the square domain is irradiated from the bottom and figure 5.3 shows the distribution when it is irradiated from the top. In both cases we can see that the maximum power is at the opposite end from the direction in which it is irradiated. Figures 5.4 and 5.5 show, the Temperature distributions in the square domain 20 seconds after irradiating and also the effect of power on the temperature distribution. Figure 5.6 shows the temperature distribution after 40 seconds.

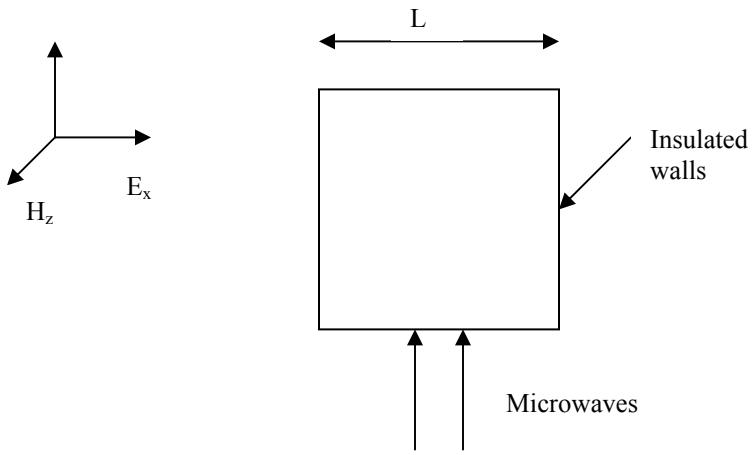

Figure 5.1 Square Cavity (L = 10) Exposed to Planes Waves

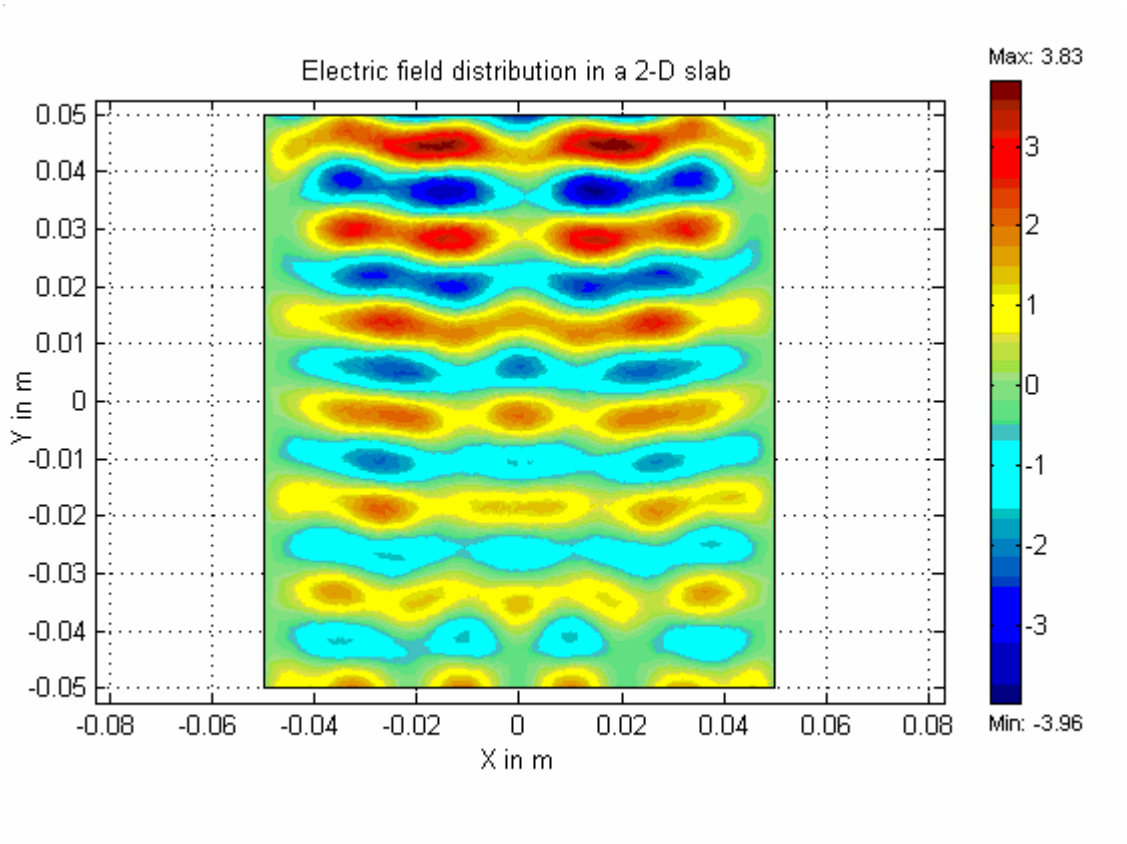

Figure 5.2 Electric Field (V/m) Distributions when Irradiated from Bottom

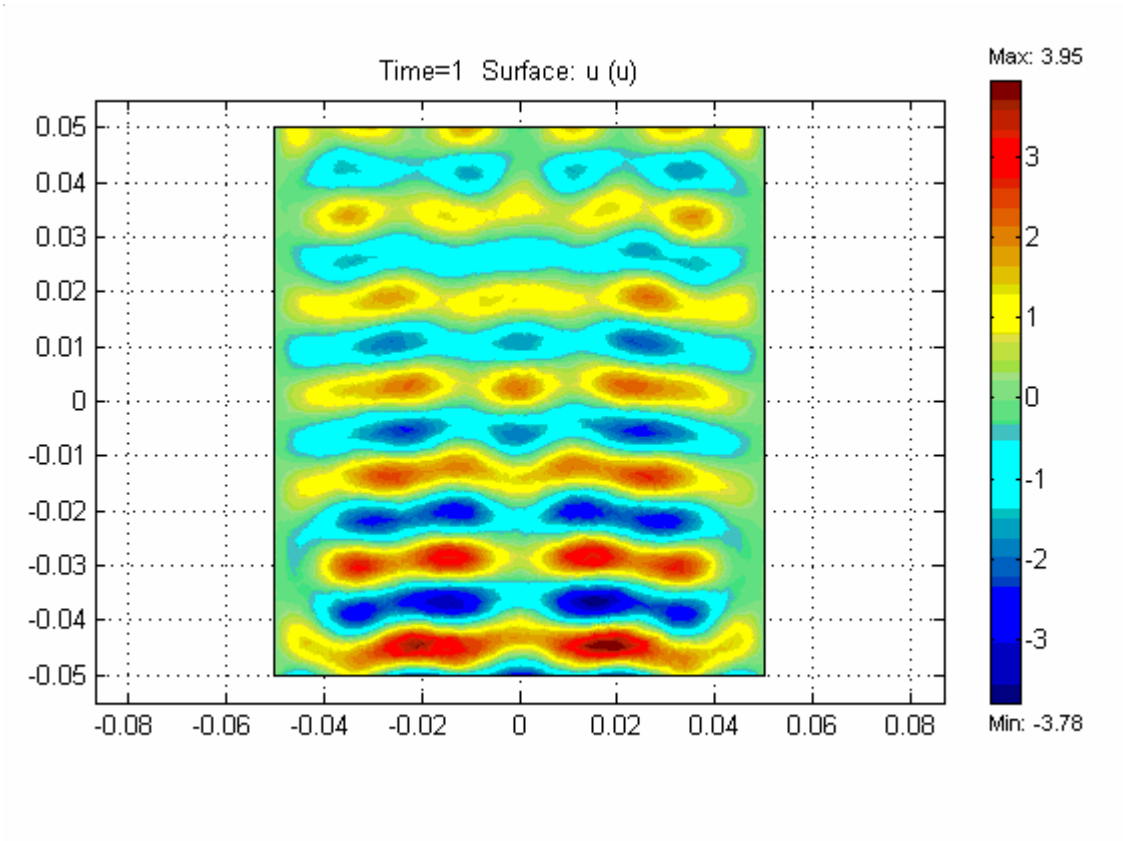

Figure 5.3 Electric Field (V/m) Distributions when Irradiated from Top

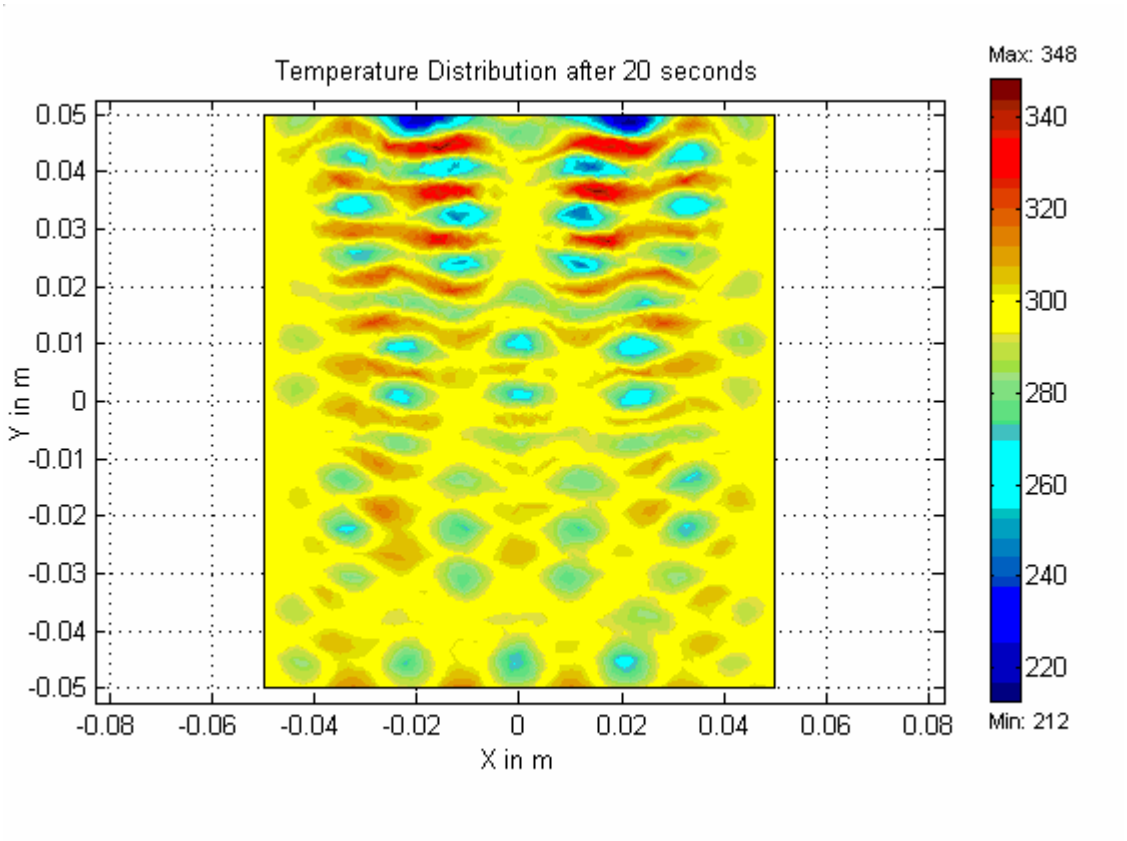

Figure 5.4 Temperature Distribution after 20 Seconds

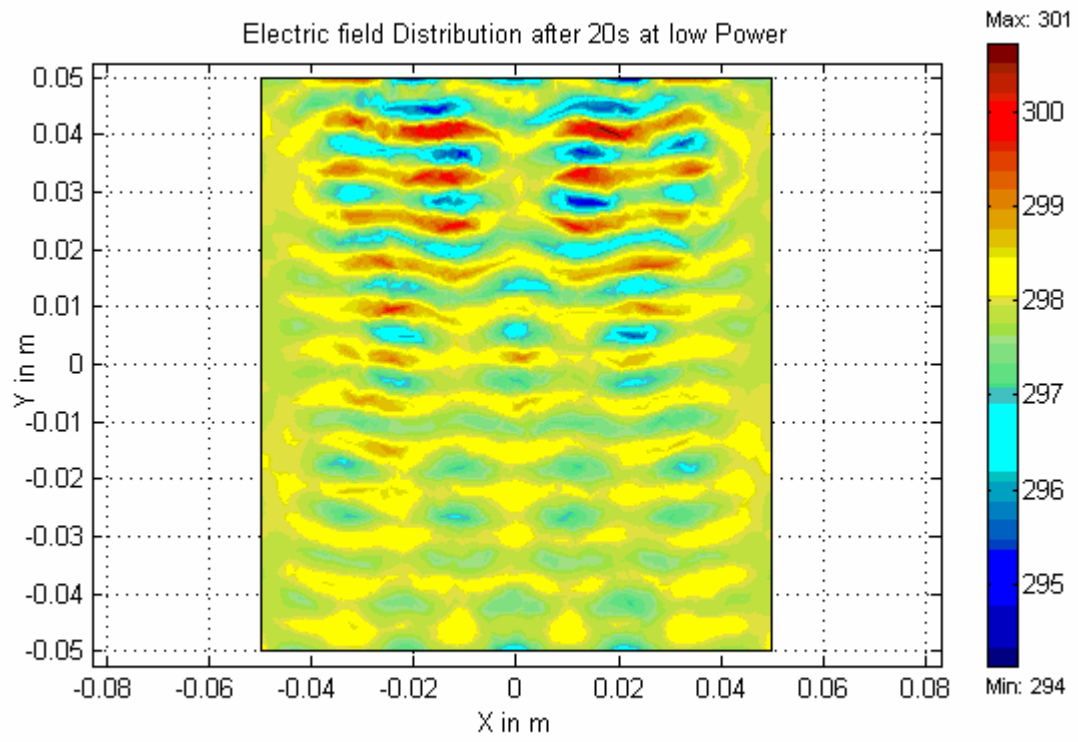

Figure 5.5 Temperature Distribution after 20 Seconds at Low Power

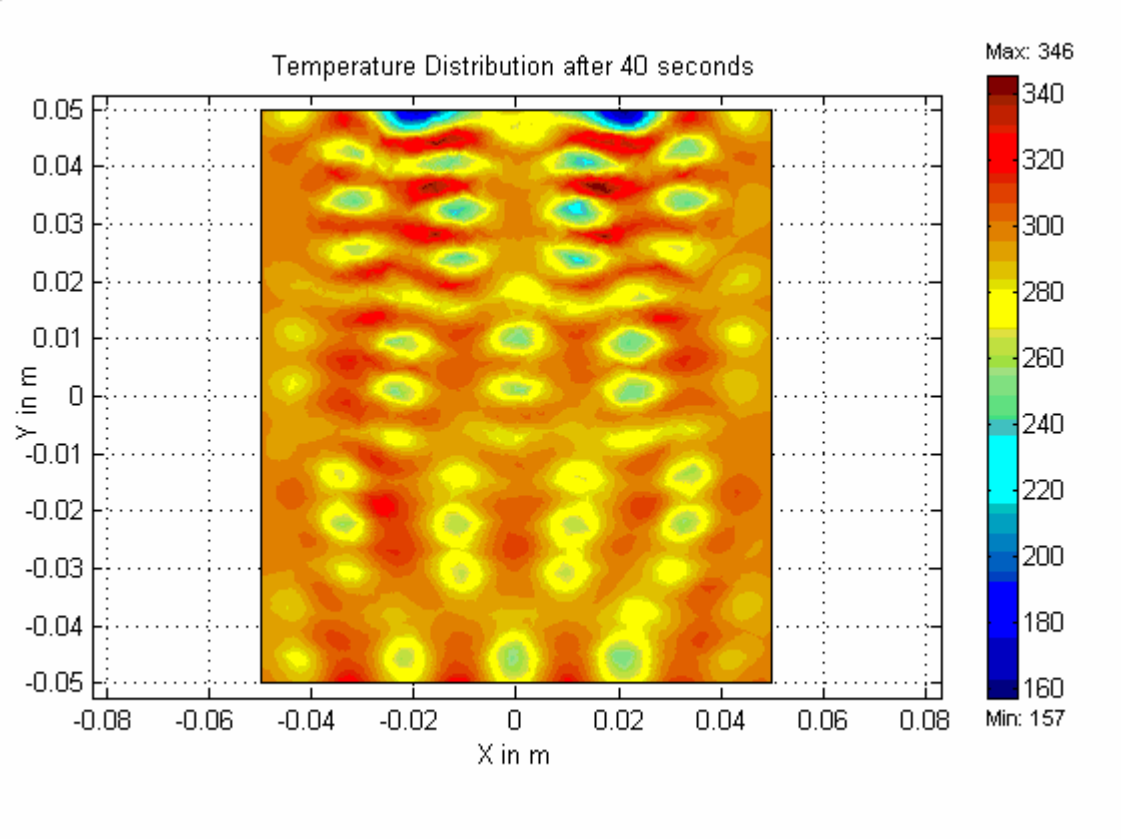

Figure 5.6 Temperature Distribution after 40 Seconds

THEORETICAL FORMULATION

Let us consider the microwave heating process of a dielectric sample. Consider a dielectric that is heated by an electromagnetic wave of frequency (ω) in the range of about 300MHz to 3GHz.

The equations governing this microwave-heating problem are the time dependent Maxwell's equations for a moving medium, the energy equation and the momentum equation (Navier-Stokes equation). Introducing the electric field **E** and the magnetic field **B**, we can obtain Maxwell equation

$$\nabla \cdot \mathbf{E} = -\nabla \cdot \mathbf{P}, \tag{6.1}$$

$$-c^{-1}\frac{\partial \mathbf{E}}{\partial t} + \nabla \times \mathbf{B} = c^{-1}\left[\frac{\partial \mathbf{P}}{\partial t} + \nabla \times (\mathbf{P} \times \mathbf{v})\right], \tag{6.2}$$

$$\nabla \cdot \mathbf{B} = \mathbf{0}, \tag{6.3}$$

$$c^{-1}\frac{\partial \mathbf{B}}{\partial t} + \nabla \times \mathbf{E} = \mathbf{0}, \tag{6.4}$$

where **P** and **v** are, respectively the macroscopic electric polarization vector and the velocity associated with the sample. In deriving these equations, we have assumed that the effect of the magnetic polarization is negligible and all the constituents are electrically neutral. The structure of **P** will be given by constitutive assumptions. We get

$$\frac{\partial \mathbf{P}}{\partial t} = \lambda(\mathbf{E} - \rho H\mathbf{P}), \tag{6.5}$$

We can determine H and λ under the condition of small deformations by restoring to theory of dielectric polarizations in which $\mathbf{P} = \chi\mathbf{E}$ is employed under $\mathbf{E} = \mathbf{E}_{\max}\exp(i\omega t)$ (Hasted, 1973; Hippel, 1954). Here, χ is the complex electric susceptibility of a dielectric ω is the frequency of the electromagnetic field and the material is at rest. We get λ and H to be

$$\lambda = \omega[im(\chi)] + \omega[re(\chi)][im(\chi)]^{-1}[re(\chi)], \tag{6.6}$$

$$H = \frac{\omega}{\rho}[\lambda]^{-1}[re(\chi)][im(\chi)]^{-1} \tag{6.7}$$

We now formulate the equations of motion for the sample on the basis of the above scheme while ignoring the multi-poles other than dipoles. The balance of mass equation for the sample is given by,

$$\frac{\partial \rho}{\partial t} + \nabla \cdot (\rho \mathbf{v}) = 0, \tag{6.8}$$

where ρ is the mass density of the sample.

The balance of linear momentum equation for the sample is given by,

$$\frac{\partial}{\partial t}(\rho \mathbf{v}) + \nabla \cdot (\mathbf{v}\rho \mathbf{v}) = \nabla \cdot \tau + \mathbf{f}_{em} + \rho \mathbf{g}, \tag{6.9}$$

$$\mathbf{f}_{em} = c^{-1}\left[c(\nabla \mathbf{E}) \cdot \mathbf{P} + (\nabla \mathbf{B}) \cdot (\mathbf{P} \times \mathbf{v}) + \frac{\partial}{\partial t}(\mathbf{P} \times \mathbf{B}) + \nabla \cdot (\mathbf{v}\mathbf{P} \times \mathbf{B}) \right], \tag{6.10}$$

here τ is the Cauchy stress, f_{em} is the electromagnetic force acting on the sample and g is the gravitational acceleration. The balance of energy can be written as

$$\rho \frac{\partial}{\partial t}(e + \frac{1}{2}\mathbf{v}^2) + \nabla \cdot \mathbf{q} = \nabla \cdot (\tau \mathbf{v}) + \rho \mathbf{f} \cdot \mathbf{v} + w_e, \tag{6.11}$$

here we denoted by e the specific internal energy, by **q** the heat flux vector and the energy production density w_e is given by

$$w_e = \mathbf{f}_{em} \cdot \mathbf{v} + \rho \mathbf{E} \cdot \frac{\partial}{\partial t}(\frac{\mathbf{P}}{\rho}), \tag{6.12}$$

using (6.8) and (6.9) we can get the reduced form of (11) to be

$$\rho \frac{\partial}{\partial t}(e) + \nabla \cdot \mathbf{q} = \boldsymbol{\tau} \cdot \mathbf{L} + \mathbf{E} \cdot \dot{\mathbf{P}} + (\mathbf{E} \cdot \mathbf{P}) \nabla \cdot \mathbf{v}, \tag{6.13}$$

where **L** is the velocity gradient.

6.1 Boundary Conditions for the Electric Field

To have a determinate model of the microwave heating process of a sample, the boundary conditions have to be furnished. The boundary conditions associated with the Maxwell field equations (6.1) through (6.4) are

$$\left|\mathbf{E}+\mathbf{P}\right|\cdot\mathbf{n}=\mathbf{0}, \tag{6.14}$$

$$\left|c^{-1}(\mathbf{E}+\mathbf{P})\times\mathbf{v}+\mathbf{B}+c^{-1}(\mathbf{v}\times\mathbf{P})\right|\times\mathbf{n}=\mathbf{0}, \tag{6.15}$$

$$\left|\mathbf{B}\right|\cdot\mathbf{n}=\mathbf{0}, \tag{6.16}$$

$$\left|\mathbf{E}-c^{-1}(\mathbf{B}\times\mathbf{v})\right|\times\mathbf{n}=\mathbf{0}, \tag{6.17}$$

These boundary conditions assume that there are no free charges at the interface between the two media. Equation 6.14 and equation 6.16 implies that the normal components of the electric fields and magnetic fields are continuous across the interface. Equations 6.15 and 6.17 indicate that the tangential components are continuous across the interface.

6.2 Boundary Conditions for the Temperature

The microwave power is a spatially distributed heat source term. If the material has temperature dependent properties then the microwave power is temperature dependent and the equations for the electric field must be solved simultaneously with the energy balance equation. If the heat is transferred from the boundaries of the sample to the surroundings by convection and radiation, the boundary condition is

$$-\mathrm{n}\cdot k\nabla T=h(T-T_{\infty})+\sigma\varepsilon(T^{4}-T_{\infty}^{4}), \tag{6.18}$$

where **n** is the outward pointing normal on the surface of the sample.

6.3 Heating in 1D

In this model the fluid velocities generated are assumed to be much smaller than the speed of light. Then the relativistic correction terms to electromagnetic equations are negligible and Maxwell's equations reduce to their standard form in a stationary medium. One more assumption would be that the time required for the fluid or heat to diffuse a wavelength is much larger than the microwave period. The later is $O(10^{-10})$ seconds for commercial microwaves. This last assumption helps in averaging all the governing equations over a microwave period. The resulting equations are a time harmonic version of Maxwell's equations and the time dependent Navier-Stokes and heat equation. The later contains the averaged microwave source term.

Within this framework, we assume that a plane time-harmonic electromagnetic wave of frequency ω impinges normally upon the fluid layer, which fills the region $0 < x < d$. A portion of this wave scatters from the interface $x = d$, a portion penetrates the layer and heats the fluid, and the remaining portion is transmitted through the other interface. Since **E**, **B** and **P** satisfy the wave equation, the electric field, which penetrates the fluid and interacts with it can be assumed in the following form,

$$\mathbf{E} = \mathbf{E}_c \cos \omega t + \mathbf{E}_s \sin \omega t \tag{6.19}$$

Similarly **B** and **P** can be written as

$$\mathbf{B} = \mathbf{B}_c \cos \omega t + \mathbf{B}_s \sin \omega t \tag{6.20}$$

$$\mathbf{P} = \mathbf{P}_c \cos \omega t + \mathbf{P}_s \sin \omega t \tag{6.21}$$

The above three substitutions are made into equation (6.1) through (6.6) and the unknown electric field is solved for using the conditions that the tangential components of both electric field and magnetic field are continuous at the boundaries.

The electric field obtained is

$$\mathbf{E} = \mathbf{E}_c \cos \omega t + \mathbf{E}_s \sin \omega t$$

where

$$\mathbf{E}_c = e^{\alpha x}(c_1 \cos \beta x + c_2 \sin \beta x) + e^{-\alpha x}(c_3 \cos \beta x + c_4 \sin \beta x) \tag{6.22}$$

and $$\mathbf{E}_s = e^{\alpha x}(c_1' \cos \beta x + c_2' \sin \beta x) + e^{-\alpha x}(c_3' \cos \beta x + c_4' \sin \beta x) \tag{6.23}$$

where α, β, c_i and $c_i^{'}$ are constants which are functions of the external electric field and the dielectric and material properties. Appendix C contains the values of these constants for water. Figure 6.1 shows the distribution of electric field in a 1-Dimensional slab of thickness 10 cm and with absorbing boundary conditions.

The next step in our modeling process would be solving the momentum and energy balance equations for the model stated above. In order to solve the heat equation one should first identify the heat source and sink terms. If we assume continuity the only additional term in the heat equation will be $\mathbf{E} \cdot \dot{\mathbf{P}}$.

From equation (6.5) and using the assumption that time required for the fluid or heat to diffuse a wavelength is much larger than the microwave period, the additional term can be simplified to,

$$\mathbf{E} \cdot \dot{\mathbf{P}} \approx \frac{\lambda \mathbf{E}^2}{1 + (\frac{\lambda \rho H}{\omega})^2} = \omega [im(\chi)] \mathbf{E}^2, \tag{6.24}$$

It can be clearly seen that the additional term in the heat equation is positive and hence it is a heat source term dependent on the electric field in the sample. This heat source term can be averaged over the microwave period to get the time-averaged heat source term thus getting rid of the time variation of the electric field.

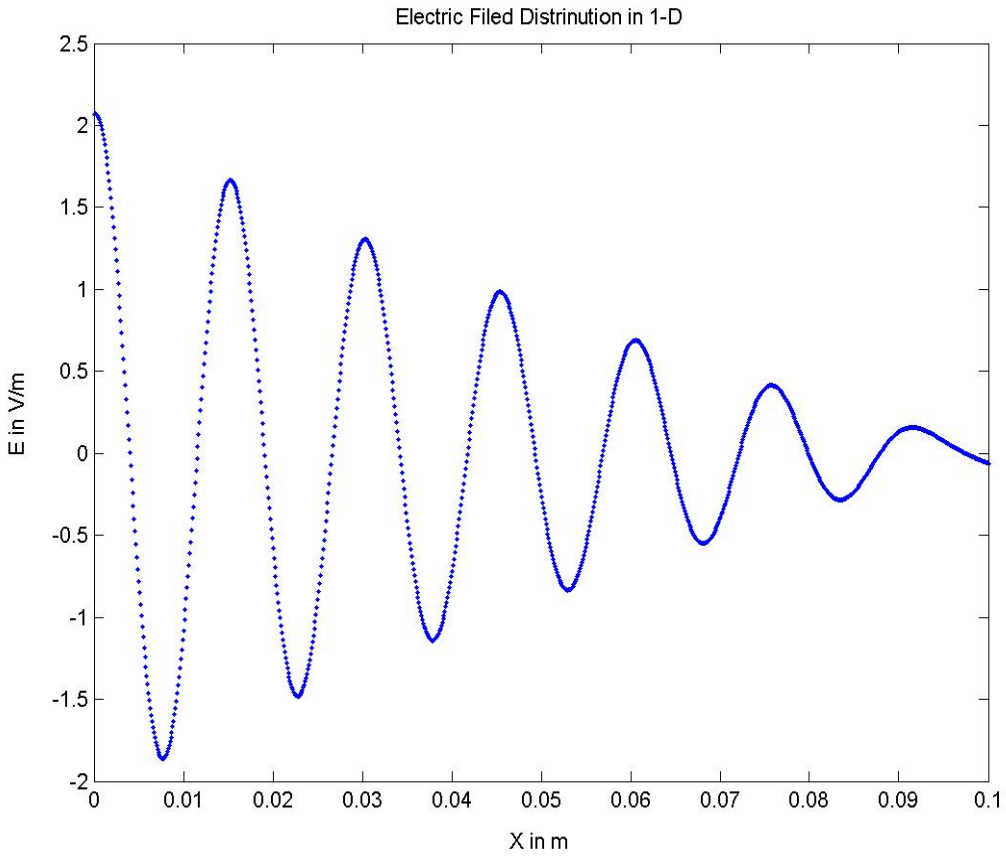

Figure 6.1 Electric Field Distribution in a 1-Dinemsional Slab

6.4 The Boussinesq Approximation:

In deriving the equations of motion for the model no assumptions were made regarding the constancy, or otherwise, of various coefficients (μ,α, k etc) which were introduced. The equations, which were derived, are, therefore, of quite general validity. But there are situations of practical occurrences (Chandrasekhar, 1961) when the variability in density and other coefficients is due to the variations in the temperature of only moderate amounts. Variations of this small amount can, in general, be ignored. But there is one important exception (Drazin and Reid, 1981): the variability of density in the body force term in the momentum equation cannot be ignored; this is because the acceleration resulting can be larger than the inertial term in the equation of motion. Accordingly the density can be treated as a constant in all the terms in the equations of motion except the one in the external force. This is the Boussinesq approximation (Chandrasekhar, 1961). For substances (Newtonian Fluids), which we shall be primarily concerned, we can write

$$\rho = \rho_0\left[1 - \alpha'(T - T_0)\right], \tag{6.25}$$

where α' is the coefficient of volume expansion and T_o is the temperature at which $\rho = \rho_o$.

6.5 Linear Stability:

Here we consider the same infinite horizontal model as above but with the two boundaries insulated; further, let there be no motions. The initial state is $T = T_o$. The basic state would be when the velocity field throughout is zero.

$$\mathbf{u} \equiv \mathbf{0}, \tag{6.26}$$

When no motions are present, the hydrodynamical equations require only that the pressure distribution is governed by the equation

$$\frac{\partial p}{\partial x} = -\rho_0\left[1 - \alpha'(T - T_0)\right]g, \tag{6.27}$$

The temperature distribution is governed by the equation

$$\rho c_p \frac{\partial T}{\partial t} = k\nabla^2 T + \omega\left[im(\chi)\right]\mathbf{E}^2, \tag{6.28}$$

The solution of equation (6.27) appropriate to the problem described is

$$T(x,t)=\frac{2T_0}{L}\sum_{m=1}^{\infty}e^{-\alpha'\beta_m^2 t}\cos(\beta_m x)\sin(\beta_m L)+\frac{\alpha'}{k}\sum_{m=1}^{\infty}\frac{1}{\alpha'\beta_m^2}(1-e^{-\alpha'\beta_m^2 t})\cos(\beta_m x)\int_0^L\cos(\beta_m x')\,f(x')dx',$$

(6.29)

Where

$$\beta_m=\frac{m\pi}{2L}$$

and *f(x)* is the time averaged heat source term.

The linear stability of the undisturbed state described above, can be analyzed by adding small perturbations $\boldsymbol{u}'$, P' and θ' and linearizing (6.13) with respect to the primed quantities to obtain:

$$\nabla\cdot\mathbf{u}'=\mathbf{0}, \tag{6.30}$$

$$\frac{\partial\mathbf{u}'}{\partial t}=-\frac{1}{\rho_0}\nabla P'+\upsilon\nabla^2\mathbf{u}'+\alpha g\theta', \tag{6.31}$$

$$\frac{\partial\theta'}{\partial t}+\mathbf{u}'\cdot\nabla\bar{T}=\frac{k}{\rho_0 c_p}\nabla^2\theta', \tag{6.32}$$

Let $t = t_o$ be the time at which the convection sets in. Making the substitution $t = t_o+\tau$ where $t \geq 0$ into (6.31) will yield

$$\frac{\partial\theta'(x,\tau)}{\partial\tau}+\mathbf{u}'\cdot\nabla\bar{T}(x,t_0+\tau)=\frac{k}{\rho_0 c_p}\nabla^2\theta'(x,\tau),$$

which can be reduced to

$$\frac{\partial\theta'(x,\tau)}{\partial\tau}+\mathbf{u}'\cdot\nabla\bar{T}(x,\tau)=\frac{k}{\rho_0 c_p}\nabla^2\theta'(x,\tau), \tag{6.33}$$

after neglecting the higher order terms after expanding.

Taking the curl of (6.30) twice we obtain the following equation involving the vertical velocity component of the fluid and the temperature:

$$\frac{\partial\Delta w'}{\partial\tau}=\alpha g\Delta_1\theta'+\upsilon\Delta^2 w', \tag{6.34}$$

where $\Delta_1 = \frac{\partial^2}{\partial y^2} + \frac{\partial^2}{\partial z^2}$. This equation along with (6.32) can be used to determine the stability of the system. It can be seen that with the functions w' and θ', known the continuity equation and using equation (6.30) the other velocity components and the perturbation in the pressure can be solved for.

Equations (6.31) and (6.32) comprise a coupled system of PDEs which can be analyzed by introducing the normal modes. We suppose that the perturbations have the forms:

$$\theta' = \Theta(x,t_0)h(y,z)e^{\sigma x}, \qquad w = W(x,t_0)h(y,z)e^{\sigma x}, \qquad (6.35)$$

The energy equation reduces to

$$\left[\sigma + \frac{\bar{T}W}{\Theta} - \frac{D^2\Theta}{\Theta}\right] = \frac{\Delta_1 h}{h},$$

which yields the Helmholtz equation $\Delta_1 h + a^2 h = 0$ for the horizontal dependence of Temperature eigenfunction. Similarly the momentum equation will yield the following eigenvalue problem depending on *a*.

$$(D^2 - a^2)((D^2 - a^2) - \sigma)W - a^2 \alpha g \Theta = 0, \qquad (6.36)$$

$$(D^2 - a^2 - \sigma)\Theta - WD\bar{T} = 0, \qquad (6.37)$$

6.6 Boundary conditions:

The fluid is confined between the planes $x = 0$ and $x = d$; on these two planes certain boundary conditions must be satisfied. Regardless of the nature of these bounding surfaces, we require

$$\frac{\partial \theta'}{\partial x} = 0 \quad \text{and} \quad w = 0 \quad \text{for} \quad x = 0 \quad \text{and} \quad x = d \qquad (6.38)$$

The above set of differential equations cannot be solved analytically but have to be solved numerically and that is out of the scope of this work. The phenomenon of exchange of stabilities has not been proven in this work but is strongly encouraged numerically

CONCLUSIONS

From the experiments it was found that the experimentally determined time constant of the thermocouple was almost the sane as the computed first order time constant. The microwave power output was used almost completely for heating since water reached the boiling point in the same time as it would reach with the maximum power output. The following conclusions were drawn from the experimental and theoretical analysis performed.

- The transient Temperature profiles for the liquids experimented were almost linear.
- The axial temperature increased with the height i.e.; the top surface heated up faster than the lower portions of the liquid in the container.
- The radial temperature values showed increasing temperature towards the center for the container size we used. The increased core heating might be due to concentration of energy or focussing by the cylindrical surface for the smaller sizes.
- The time response did not show any significant variation with the position of the sample inside the microwave cavity.
- The effect of microwave power was studied. The response showed the on-off functioning of the microwave power at lower powers and hence more heating time to reach the same temperature.
- The height of the sample in the oven did not have any significant effect on the sample since there wasn't much variation in the time response.
- The slope of the time response curve in the case of pure water was somewhat more than in the case of cornstarch solution. Steady state couldn't be reached within 3 minutes of heating time. The solution cooked and expanded so enough data couldn't be recorded. The time response of cornstarch solution wasn't as uniform as water. This might be because of the solidification and expansion of cornstarch solution.
- Tomato ketchup appeared to heat at much faster rate than water and cornstarch. This can be attributed to the difference in internal electric field and differences in material and electric properties.
- 2-D numerical simulations were done to observe the temperature and electric field variation in a square cavity containing water. A wave like distribution for the electric

field was observed with the maximum electric field at the opposite end from which the cavity was irradiated. The temperature was also maximum at that end.

- A general theoretical model was developed for microwave heating process and 1-D boundary value problem was solved for electric field and Temperature.
- Stability analysis was done one a 1-D model and the equations of perturbation were derived.

LITERATURE CITED

Ayappa, K. G and Basak, T., "Role of Length Scales on Microwave Thawing Dynamics in 2-D Cylinders", *Int. J. Heat and Mass Transfer*, **45**, 4543-4549 (2002).

Ayappa, K. G and Basak, T., "Influence of Internal Convection During Microwave Thawing of Cylinders", *AIChE J.,* **47**, 835 (2001).

Ayappa, K. G and Basak, T., "Analysis of Microwave Thawing of Slabs with Effective Heat Capacity Method", *AIChE J.,* **43**, 1662 (1997).

Ayappa, K. G., Davis, H. T., Davis, E. A., & Gordon, J., Barringer, S. A., "Effect of Sample Size on Microwave Heating Rate: Oil Vs Water", *AIChE J.,* **40**, 1433 (1994a).

Ayappa, K. G., Davis, H. T., Davis, E. A., & Gordon, J., "On Microwave Driven Convection in a Square Cavity", *AIChE J.,* **40**, 1268 (1994b).

Ayappa, K. G., Davis, H. T., Davis, E. A., & Gordon, J., "2-D Finite Element Analysis of Microwave Heating", *AIChE J.,* **38**, 1577 (1992).

Ayappa, K. G., Davis, H. T., Davis, E. A., & Gordon, J., "Analysis of Microwave Heating of Materials with Temperature Dependent Properties", *AIChE J.,* **37**, 313 (1991a).

Ayappa, K. G., Davis, H. T., Crapiste, G., Davis, E. A., & Gordon, J., "Microwave Heating: An Evaluation of Power Formulations", *Chemical Engineering* S*cience,* **46**(4), 1005-1016, (1991b).

Barringer, S. A., E. A. Davis, J. Gordon, K.G. Ayappa and H. T. Davis, " Microwave Heating Temperature Profiles for Thin Slabs Compared with Maxwell's and Lambert's Law Predictions", *J. Food Sci*., **60**, 1137 (1995).

Barringer, S. A., E. A. Davis, J. Gordon, K.G. Ayappa and H. T. Davis, "Effect of Sample Size on Microwave Heating Rate: Oil vs. Water", *AIChe J*., **40**, 1433 (1994).

Chandrasekhar S., *Hydrodynamic and Hydromagnetic Stability*, Dover Publications Inc., New York, (1961).

Chen, D. D., Singh, R. K., Haghighi, K. & Nelson, P. E. "Finite Element Analysis of Temperature Distribution in Microwaved Cylindrical Potato Tissue". *J. Food Sci*., **18,** 351-368, (1993).

Clemens, J. & Saltiel, C., "Numerical Modeling of Materials Processing in Microwave Furnaces". *International Journal for Heat and Mass Transfer*. **39** (8), 1665-1675, (1995).

Datta, A. K. and Prosetya, H., "Batch Microwave Heating of Liquids: An Experimental Study", *J. of Microwave Power and Electromagnetic Energy*, **26**, 215 (1991).

Datta, A. K., Prosetya, H. and Hu, W., "Mathematical Modeling of Batch Heating of Liquids in a Microwave Cavity", *J. of Microwave Power and Electromagnetic Energy*, **26**, 38 (1992).

Datta, A. K. & Zhang, H. (2000). Coupled Electromagnetic and Thermal Modeling of Microwave Oven Heating of Foods. *International Microwave Power Institute.* **35**(2)*,* 71-85.

Drazin, P. G., Reid, W. H., *Hydrodynamic Stability*, Cambridge University Press, New York, (1981).

Gartling, D. K., "A Finite Analysis of Volumetrically Heated Fluids in an Axisymmetric Enclosure", in *Finite Element in Fluids*, 4, John Wiley and Sons, NY, (1982).

Gartling, D. K., "Convective Heat Transfer Analysis by Finite Element Method", *Computational Methods in Applied Mechanics and Engineering*, **12**, 365-382 (1977).

Haala, J. & Wiesbeck, W., "Simulation of Microwave, Conventional and Hybrid Ovens Using a New Thermal Modeling Technique", *Journal of Microwave Power,* **35**(1)*,* 34-43, (2000).

Hasted, J. B., *Aqueous Dielectric*, Chapman and Hall, London, 1973.

Hippel Von, A. R., *Dielectric and Waves*, The MIT Press, Cambridge, Massachusetts, 1954.

Jahn, M. and H. H. Reineke, " Free Convection Heat Transfer with Internal Heat Source Calculations and Measurements", in *Proc. 5th Int. Heat Transfer Conf*., Tokyo, Japan, **3**, 74 (1970).

Lambha, N. K., Korpela, S. A. and Kulacki, F. A., "Thermal Convection in a Cylindrical Cavity with Uniform Volumetric Energy Generation", in *Proc. 6th Heat Trans. Conf.*, Toronto, Canada, **2**, 311 (1978).

Lin, Y. E., Anantheswaran, R. C., Puri, V. M. & Yeh, G., "Finite Element Modeling of Heat and Mass Transfer in Food Materials During Microwave Heating-Model Development and Validation", *Journal of food engineering.* **25,** 509-529, (1995).

Mudgett, R. E., "Microwave Properties and Heating Characterisics of Foods", *Food Technol*. **6**, 84 (1986).

Ohlsson, T. and N. E. Bengtsson, "Microwave Heating Profiles in Foods- A Comparison Between Heating Experiments and Computer Simulation", *Microw. Energy Appli. Newsl*. **6**, 3 (1971).

Ohlsson, T. & Risman, P. O., "Temperature Distribution of Microwave Heating-Spheres and Cylinders", *Journal of Microwave Power,* **13**(4), 303-310, (1978).

Oliveira, M. E. C. & Franca, A. S., "Microwave Heating of Food Stuffs", *Journal of Food Engineering.* **54**, 347-359, (2002).

Oliveira, M. E. C. & Franca, A. S., "Finite Element Analysis of Microwave Heating of Solid Products", *International communication for Heat and Mass Transfer,* **27**(4), 527-536, (2000).

Rajagopal, K. R and Wineman, A. S., "Flow of Electrorheological Materials", *Acta Mechanica,* **91**, 57-75 (1992).

Rajagopal, K. R and Tao, L., "Modeling of the Microwave Drying Process of Aqueous Dielectrics", *Z. angew. Math. Phys*, **53**, 923-948 (2002).

Zhao, H. & Turner, I. W., "The Use of a Coupled Computational Model for Studying the Microwave Heating of Wood", *Applied Mathematical Modeling*, **24,** 183-197, (2000).

APPENDIX A

NOMENCLATURE

B magnetic field A/m

c velocity of light in free space, m/s

c_p specific heat capacity, J/kg/K

e specific internal energy

E electric field, V/m

f_{em} electromagnetic force, N

g acceleration due to gravity, m/s^2

k coefficient of thermal conductivity, W/ (m.K)

L velocity gradient, s^{-2}

P macroscopic electric polarization

p pressure, N/m^2

q heat flux vector, W/m^2

T_o reference temperature, K

v velocity, m/s

Greek Symbols

ρ density, kg/m^3

ν kinematic viscosity, m^2/s

χ complex dielectric susceptibility

ω electromagnetic wave frequency, Hz

β' coefficient of volume expansion, K^{-1}

τ Cauchy stress. N/m^2

APPENDIX B

PROPERTIES/CONSTANTS	VALUE
DENSITY	1000 Kg/m^3
VISCOSITY	8.94 E-4
THERMAL CONDUCTIVITY	0.61W/ m K
HEAT TRANSFER COEFFICIENT	44 W/ m^2K
ACCELARATION DUE TO GRAVITY	9.8 ms^{-2}
DIELECTRIC SUSCEPTIBILITY	403+10.43i
FREQUENCY	2*pi*2.45E9 Hz
PERMEABILTY	8.85E-12 F/m
ELECTRIC FIELD	475.49 V/m
SPECIFIC HEAT	4180 J/Kg K
COEFF OF VOLUME EXPANSION	5.344E-4 K^{-1}
AMBIENT TEMPERATURE	298 K
DIELECTRIC CONSTANT	66
DIELECTRIC LOSS FACTOR	3.5

APPENDIX C

CONSTANT	VALUE
C1	-0.263
C2	2.3291
C3	0.0122
C4	0.1943
$C1^{'}$	0.0122
$C2^{'}$	-0.1943
$C3^{'}$	0.263
$C4^{'}$	2.3291
α	11.0494
β	417.01

VITA

Bhagat Chandra Kota was born in Munagala, India on 8th October 1979. He received his Bachelor of Technology degree in chemical engineering from the Indian Institute of Technology, Madras, India in May 2001. The author may be contacted at 1-6-102/3/1 Ramalingeshwara Theater, Suryapet, Nalagonda Dist, Andhra Pradesh, 500036 or by email at bhagat@neo.tamu.edu.